PROD. TYPE: COM
PP: 1-21 (col.fig.: nil)
HE2611 MODE+
ED: Smitha Gowda
PAGN: Jagan – SCAN: Global

ARTICLE IN PRESS

Available online at www.sciencedirect.com
ScienceDirect
International Journal of Hydrogen Energy ▮▮▮ (▮▮▮▮) ▮▮▮–▮▮▮
International Journal of HYDROGEN ENERGY
www.elsevier.com/locate/ijhydene

Baseline model of a centralized pv electrolytic hydrogen system

James E. Mason[a,*], Ken Zweibel[b]

[a]*Hydrogen Research Institute, 52 Columbia Street, Farmingdale, NY 11735, USA*
[b]*PrimeStar Solar, 1740 Skyway Drive, Suite B, Longmont, CO 80504, USA*

Received 26 August 2006; received in revised form 16 December 2006; accepted 17 December 2006

Abstract

This study performs an economic and environmental analysis of a centralized pv electrolytic hydrogen system scaled to supply H_2 to one million light duty vehicles and light commercial trucks. Annual H_2 production is 217-million kg. The size of the pv electrolysis plant to produce this quantity of H_2 is a 5.12-$GW_{dc\text{-}in}$ electrolysis plant and a 6.0-GW_p pv power plant. The land area of the pv electrolysis plant is 260 km^2. The total capital costs of the pv electrolysis H_2 system is $12.4 billion. The levelized H_2 pump price estimate is $6.48/kg. The life cycle primary energy use is 36 MJ/kg of H_2 consumption, and life cycle CO_2 equivalent emissions are 2.6 kg/kg of H_2 consumption. The replacement of conventional gasoline powered vehicles with H_2 powered vehicles reduces primary energy use and CO_2 emissions by 90%.

Keywords: Hydrogen; Solar; Photovoltaics; Electrolysis

1. Introduction

This study is an economic and environmental analysis of a centralized electrolytic hydrogen (H_2) system using photovoltaic (pv) electricity, long-distance pipelines, and metal hydride (MH) H_2 storage containers for local distribution. The objective is to establish baseline economic and CO_2 emissions parameters for a pv electrolytic H_2 system to compare to other types of H_2 production and distribution systems. The model includes estimates of capital investments, levelized H_2 prices, and life cycle primary energy use, CO_2 emissions, and resource utilization. The study is important because it advances knowledge about an energy source that can help alleviate the most serious consequences of global warming and the emerging global oil supply/demand imbalance.

The pv electrolytic H_2 production and distribution system is scaled in size to support the operation of one million H_2 powered vehicles. At this H_2 volume, prior research indicates that long distance pipeline is the lowest cost method of H_2 distribution [1]. The construction of 1000 km of H_2 pipeline for the development of an integrated pipeline network is coupled to each scaled pv electrolysis plant. Also included in the pv H_2 system model are four city gate distribution centers and 1000 H_2 refueling stations for each scaled pv electrolysis plant. The local distribution system distributes H_2 by truck in MH storage containers. In addition, it is assumed that H_2 vehicles have MH fuel tanks. While MH H_2 storage containers and vehicle fuel tanks are still in the research stage of development [2], they are one of the preferred means of H_2 storage being evaluated [3]. The investigation of MH H_2 storage increases the knowledge base of local H_2 storage and delivery systems [1].

The presentation begins with a detailed description of the pv electrolytic H_2 production and distribution system. This is followed by a methodology section, which presents data sources and the methods used to estimate levelized H_2 prices and life cycle energy use, CO_2 emissions, and resource utilization. Research findings and sensitivity analyses are presented in Section 4. As an alternative to pipelines, distributed electrolysis plants located in proximity to urban H_2 using pv electricity delivered by power lines are evaluated in Section 5, and the findings are compared to the findings for the centralized pv electrolytic H_2 system with pipelines. The study concludes with a summary of findings and suggestions for further research.

* Corresponding author. Tel.: +1 516 694 0759.
E-mail addresses: hydrogenresearch@verizon.net (J.E. Mason), Ken_Zweibel@primestar.com (K. Zweibel).

0360-3199/$ - see front matter © 2007 International Association for Hydrogen Energy. Published by Elsevier Ltd. All rights reserved.
doi:10.1016/j.ijhydene.2006.12.019

Please cite this article as: Mason JE, Zweibel K. Baseline model of a centralized pv electrolytic hydrogen system. Int J Hydrogen Energy (2007), doi: 10.1016/j.ijhydene.2006.12.019

2. Description of the pv electrolytic H_2 production and distribution system

2.1. H_2 production

The annual fuel consumption of one-million H_2 powered vehicles with an average vehicle fuel economy of 88 km/kg H_2 and an average travel distance of 17,700 km/year/vehicle is 202-million kilograms of H_2 per year.[1] Annual H_2 production is 217-million kg/year, which is 7% greater than H_2 consumption to cover 3% losses from distribution leakage, for H_2 to power electrolyser plant, pipeline, and city gate compressors, and for city gate H_2 delivery trucks. The 3% H_2 leakage rate is twice the natural gas leakage rate [4].

The pv electrolysis plants are to be built at locations receiving at least an average solar radiation (insolation) level of 271 W/m^2 to maximize the operating capacity factor of electrolysers. With this insolation level, the pv power plant and the electrolysis plant are able to produce electricity and H_2 at a average daily rate of 6.5 h of peak production, which is an annual 26% average capacity factor for the pv power plant.[2] Areas of the world with high insolation levels are presented in Fig. 1.

The rated power of the pv power plant is 6-GW$_p$. The pv power plant supplies electricity to the electrolysers, the electrolysis plant low-pressure screw-type compressors, and the high-pressure reciprocating compressors for the pipeline compression station. In addition, pv electricity is used for water pumps, water distillation, water cooling, and administration and maintenance buildings.

The electricity output of pv power plants decreases over time because of module soiling, pv module output degradation, and catastrophic pv module failures. To maintain a constant level of electricity output, the design of the pv power plant includes the annual installation of new pv to compensate for pv electricity output losses. The pv module degradation and soiling is assumed to decrease pv electricity output at a constant rate of 1.0% per annum over the operating life of pv modules. Catastrophic pv module failure, which are caused by factors such as manufacturing defects, glass stress fractures, and lightning strikes, is assumed to be 0.01% per annum. The financial accounting for the annual pv additions is a normal operating and maintenance expense.

At present, thin film pv is the only pv technology clearly demonstrating the potential to meet the combined baseline module cost, \$60/m^2, and baseline performance, 10% pv module efficiency needed to make the ¢/kW h system goals for this study [5].[3] The combination of module performance and cost for other pv technologies (e.g., wafer silicon) are not as economical at the system level. Over time, additional pv technologies are expected to meet the pv cost and performance projections, and existing ones are expected to continue their cost reductions and efficiency improvements.

The baseline projections of this study assume a 30 year pv module operating life. However, it is quite plausible, but not verifiable with present data, that the operating life of pv will be 60 years with a 1% annual degradation rate (and the degradation rate improve in the future). This study includes two models for Years 31–60 H_2 production, one model with a 30 year pv module operating life and the other model with a 60 year pv module operating life. In both cases, the balance of the pv system (mounting frames, wiring conduct, etc.) is assumed to be retained for the full 60 years. The analysis of H_2 production costs with 60 year pv module operating life is performed to provide a range in what can be realistically expected with future developments.

While a variety of electrolyser technologies are currently marketed, the type of electrolyser with a demonstrated ability to meet the cost and performance projections of this study are atmospheric, bi-polar, alkaline electrolysers [6]. Alkaline electrolysers have a long track record for dependability, low-cost maintenance, and long operating life. The operating life of electrolysers is affected by the utilization rate [7]. With the low 26% capacity factor of pv electrolysis plants, the electrolyser operating life is 60 years [8]. At the 26% capacity factor electrolyser maintenance costs are reduced, since the nickel replating cycle of electrolyser cells and electrodes only occurs every 12 years rather than the normal seven years with electrolyser capacity factors of 80% or greater.

2.2. H_2 distribution

Atmospheric electrolysers produce H_2 at an outlet pressure of 0.1 MPa. After the H_2 has been dried and purified, it is compressed and transported to a pipeline compressor station. At the electrolysis plant, screw-type compressors compress the H_2 to 0.8 MPa for transport to the pipeline compression station. The compression station has high pressure reciprocating compressors, and the H_2 is compressed from an inlet pressure of 0.69 MPa to a pipeline pressure of 6.9 MPa for long distance transport to city gate distribution centers and regional underground H_2 storage facilities.

H_2 pipelines and compressors have to account for the low density and viscosity of H_2 . Pipe welds and compressor seals, valves, gaskets and fittings have to be extra-secure to prevent H_2 leakage, which increases the cost of H_2 pipelines and compressors relative to those for natural gas delivery systems. It

[1] It is assumed that the adoption of H_2 as a transportation fuel is contingent its use by advanced fuel economy vehicles. The only vehicles with a fuel economy of 88 km/kg H_2 are fuel cell vehicles (FCV) and advanced hybrid electric vehicles (HEV), which include plug-in HEV models.

[2] Peak insolation is defined as 1000 W/m^2 of surface area. A location with an average daily insolation level of 271 W/m^2 receives on average 6504 W h/m^2 of sunlight per day (271 W × 24 h). Dividing this by 1000 W/m^2 gives the 6.5 h of daily peak insolation. The rating of pv modules in terms of watts of electricity output are evaluated under the standard operating conditions of 1000 W/m^2, e.g., a 100-W$_p$ pv module produces 100 W of electricity under peak sunlight conditions, which subscript p indicates.

[3] It is assumed that 10% efficient thin film pv modules will be available for the first large pv electrolysis plants, and over time pv modules with higher efficiencies will become available. At present, the best efficiency for a thin film pv module being produced at the > 50 MW$_p$/year scale is 9.4%. While some thin film pv modules with efficiencies > 12% have been produced on a small scale, there are numerous technical challenges in maintaining high efficiency levels while scaling-up pv manufacturing capacity.

Please cite this article as: Mason JE, Zweibel K. Baseline model of a centralized pv electrolytic hydrogen system. Int J Hydrogen Energy (2007), doi: 10.1016/j.ijhydene.2006.12.019

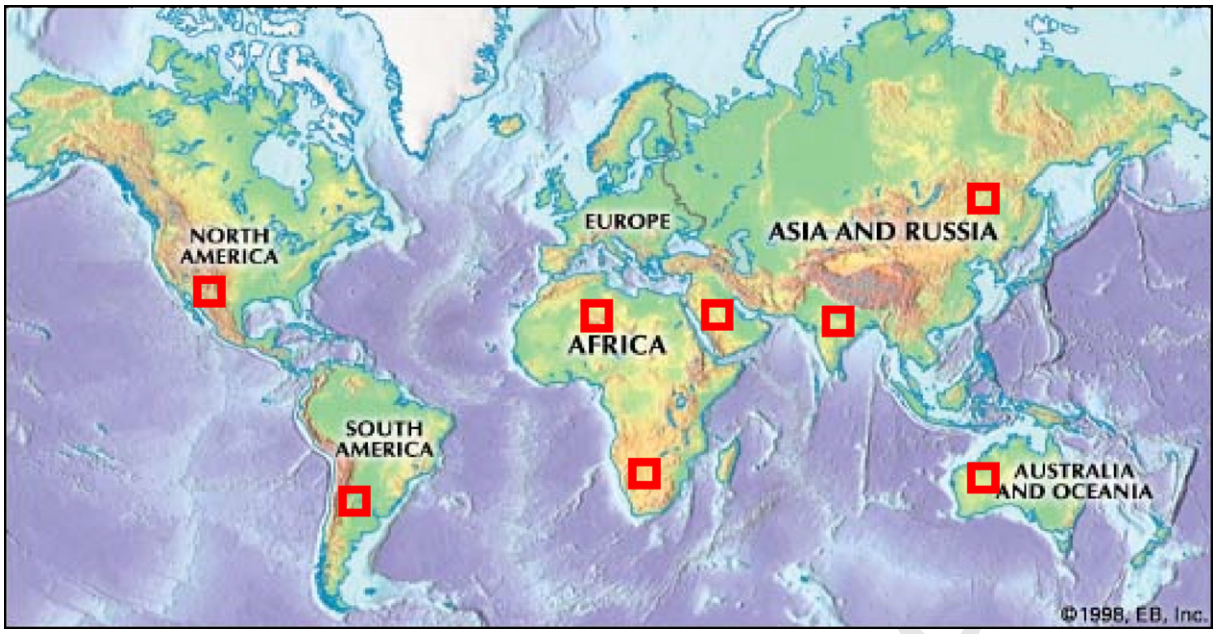

Fig. 1. Areas in boxes are regions with high average insolation levels. (Copyright permission granted by Encyclopedia Britannica.)

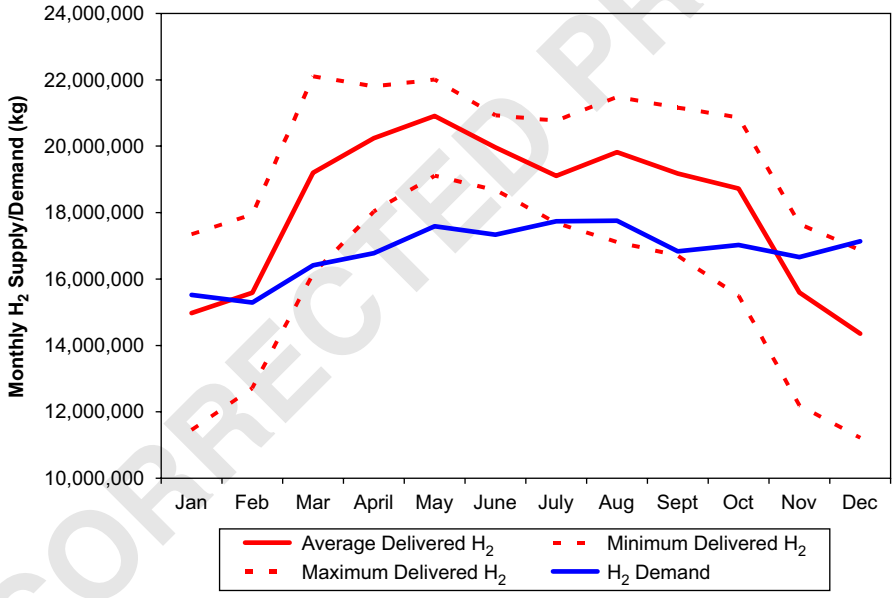

Fig. 2. Monthly H_2 production and fuel demand (one-million H_2 vehicles). *Notes*: a. Monthly H_2 demand is derived from a multi-year average of gasoline consumption in the US from US Federal Highway Administration (2003) data [9]. Average monthly H_2 production levels are based on averages of six locations in the southwest US with data from NREL's Solar Radiation Data Manual for Flat-Plate and Concentrating Collectors [10]. b. Correlation between average monthly H_2 supply and monthly H_2 demand is 0.61.

is assumed that the capital investments for H_2 pipelines and compressors are ~50% greater than the capital investments for natural gas delivery systems.

Pipeline booster compressors are installed to control the pipeline H_2 flow rate to city gate distribution centers. Because of friction and gravity, pipeline pressure decreases with distance traveled. A pressure drop of 1.4 MPa per 100 km is assumed for this analysis. Actual pressure drop is contingent on pipeline characteristics and terrain. Booster compressors are placed at 100 km intervals to maintain pipeline pressure and the H_2 flow rate.

Seasonal variation in insolation levels creates seasonal variation in pv electrolytic H_2 production. Also, there is seasonal variation in vehicle fuel demand. The relationship between average monthly pv electrolytic H_2 production and average monthly vehicle fuel demand is presented in Fig. 2. To insure an ade-

Please cite this article as: Mason JE, Zweibel K. Baseline model of a centralized pv electrolytic hydrogen system. Int J Hydrogen Energy (2007), doi: 10.1016/j.ijhydene.2006.12.019

quate supply of H_2 at all times, H_2 is stored in underground storage facilities at depleted natural gas fields and salt or rock caverns. Notice in Fig. 2 that H_2 production is less than demand from mid-October through February. The storage of 35-million kg of H_2, which is sufficient to supply two months of peak H_2 demand, is used to maintain local supply levels during the low H_2 production period. Underground storage facilities are designed for one annual cycle of withdrawals and injections. Withdrawals are from mid-October through February, and injections are from late-February through early June.

It is assumed that the 1000 km of pipeline allocated per pv electrolysis plant is an extension to a regional H_2 pipeline network. To maintain desired pressures, pipeline H_2 booster compressors are located at 60 mile intervals. With the construction of an integrated pipeline network, H_2 can be supplied to markets thousands of kilometers from the electrolysis plants.

The construction of five pv electrolysis plants with the allocation of 5000 km of pipeline can provide H_2 for five million vehicles in local markets comprising six of the top 10 largest cities in the US, 11 of the 12 largest cities, and 25 of the 100 largest standard metropolitan areas. A pipeline system extending from electrolysis plants in west Texas and New Mexico can supply H_2 to the East Coast, Florida, and the south-central US. A pipeline system extending from electrolysis plants in the California/Arizona/Nevada border areas can supply H_2 throughout southern California, northern Arizona, and southern Nevada. A pipeline system extending from electrolysis plants in New Mexico can supply H_2 to markets east of the Rockies.

City gate distribution centers receive H_2 from the pipeline, and then load the H_2 into MH containers for truck delivery to local H_2 refueling stations. MH storage is selected for this study because an automotive company representative in a personal interview stated that MH storage is preferred to compression of H_2 at 68.95 MPa, which is the required fuel tank H_2 storage pressure to achieve an acceptable vehicle driving range [11]. Another reason for the choice of a MH storage system is because of a lack of research on MH storage systems for local H_2 distribution [1].

The MH containers are assumed to weigh 33,334 kg and to hold 2000 kg of H_2, which is a 6% H_2/MH ratio by mass.[4] The typical highway weight limit for tractor/trailer trucks is 36,000 kg. Therefore, the MH containers can be transported by truck from the city gate distribution centers to filling stations. Empty MH containers at the filling stations are returned to the city gate distribution centers for refill. The recharging pressure of the MH containers and vehicle MH tanks is 11.7 MPa [13].

There are 1000 filling stations, with each station servicing an average of 1000 H_2 powered vehicles. Each filling station has one 10-kW compressor, two H_2 dispensers, two MH container stands and one MH container from which vehicles with MH fuel tanks are refueled. The second container stand is for container replacement. Average daily demand for H_2 is 590 kg of H_2, and H_2 deliveries are made every 3–4 days.

3. Methodology

3.1. H_2 system cost and performance estimates

Cost estimates, performance parameters, and operating life of the central components of a pv electrolytic H_2 system are listed in Table 1. All component cost estimates are based on an optimized manufacturing scale. The pv cost estimates are from Zweibel [5] and Keshner and Arya [14]. The pv performance parameters of pv electrolysis plants are informed by studies of the solar hydrogen project at Neunburg vorm Wald, Germany [6,15]. The cost and performance parameters of electrolysers are from the collaborative study of distributed, grid-connected electrolysis plants by Norsk Hydro and Electricité de France [7].[5] The cost estimates for H_2 compressors are from Amos [16]. The pipeline cost estimates are approximately ~50% higher than the estimates of Yang and Ogden [1]. A conservative estimate of pipeline cost is adopted for this study to provide a cushion for uncertainty regarding actual pipeline distances to insure H_2 delivery to all local distribution centers within the pipeline network. Monetary units are stated in 2006 US $.

3.2. Calculation of levelized H_2 price

H_2 price estimates are levelized prices and are estimated by the net present value cash flow method to assess capital budgeting projects [17]. This method differs from accounting net present value methods. The levelized H_2 price estimate for this study is derived by finding the H_2 price that creates a zero net present value for the sum of discounted annual net cash flows over the investment period. The capital budgeting definition of net cash flow is after-tax cash flows from operations discounted at the present value of the cost of capital. The net present value formula is

$$\mathrm{NPV} = \sum_{t=1}^{N} \frac{\mathrm{NCF}_t}{(1+k)^t} - I_0, \qquad (1)$$

where NPV is the net present value of the investment project, NCF_t the net cash flows per year for the project, k the cost of capital, which is a weighted average cost of capital (WACC), $(1+k)^t$ the discount rate to convert annual net cash flows to their

[4] This study assumes a MH with a 6% H_2 reversible storage by weight. Jorgenson [3] states that HRL working with GM has achieved 9% H_2 reversible storage by weight with a lithium-boro hydride and magnesium hydride mixture, but the operating temperature of 275 °C is higher than they would like. A magnesium lithium ($LiNH_2/MgH_2$) hydride has achieved 4.3% H_2 reversible storage by weight at an operating temperature of 200 °C [12]. Hence, the 6% H_2 storage by weight estimate of this study seems reasonable.

[5] Cloumann et al. [7] study of electrolytic H_2 production is based on the use of grid-distributed electricity. The electrolysis performance efficiency of 72% from the Cloumann et al. study is a global efficiency and includes the energy to compress H_2 to a pressure of 33 bar, H_2 losses in the drying/purification phases, and the energy for pumping water and KOH. In contrast, this study models compression and pumping energy separately and assumes an electrolysis efficiency of 76%. The installed cost for the Norsk electrolysis plant with a H_2 production capacity of 4200 kg/h is $800/$kW_{dc\text{-}in}$ (2005 US $), which is 23% higher than the electrolysis plant cost in this study.

Please cite this article as: Mason JE, Zweibel K. Baseline model of a centralized pv electrolytic hydrogen system. Int J Hydrogen Energy (2007), doi: 10.1016/j.ijhydene.2006.12.019

Table 1
H_2 system cost and performance assumptions for 2010–2015 pv electrolysis plants

	Parameters	Operating life (years)
(A) pv power plant		
1. pv area cost ($/m^2)	$60/m^2	30 or 60
a. Freight charges @ $142/short ton	$2/m^2	
b. Year 31 pv area cost ($/m^2)	$50/m^2	30
2. pv module efficiency (1st generation)	10%	
a. Year 31 pv module efficiency	12%	
3. pv balance of system (BOS) costs	$50/m^2	60
a. Freight charges @ $100/short ton	$2/m^2	
b. Year 31 BOS (only labor costs—40% of BOS)	$20/m^2	30
4. DC/DC converters	$75/kW$_{dc-in}$	30
5. pv system net efficiency (DC output per W_p installed)[a]	85%	
a. Losses from wiring, ambient heat, module mismatch, etc.	−11%	
b. Losses from dc/dc converters and coupling to electrolysers	−4%	
6. pv system availability (included in pv system efficiency)	99%	
7. Average hours/day of peak insolation @ 271 W/m^2 insolation	6.5 h/day	
8. O&M expenses including pv additions (% of capital cost)	1.0%	
9. Land cost ($/ha)	$2500	
10. Property taxes (% of capital)[b]	0.5%	
(B) Electrolysis plant		
1. Electrolysers (including dc–dc power conditioning)	$425/kW$_{dc-in}$	60
2. Electrolyser efficiency net (energy in/H_2 energy out)	76%	
3. Electrolyser availability	98%	
4. Electrolyser capacity factor	26.5%	
5. Compressors (low pressure, water injected, screw type)	$340/hp	30
a. Compressor efficiency	70%	
6. Water system (collection, pumping, purification)	$5,000,000	60
7. Administration, maintenance, and security buildings	$10,000,000	60
8. Electrolysis plant annual O&M expenses (% of capital cost)	2.0%	
9. Property taxes (% of Capital)	0.5%	
(C) Other H_2 system components		
1. Pipeline	$1,242,800/km	60
2. Pipeline compressors (reciprocating)	$670/hp	40
a. Compressor efficiency	70%	
3. Pipeline booster compressors (intervals)	97 km	40
4. Metal hydride (MH) H_2 storage capital cost	$30/kg MH	30

[a]Annual pv additions replace electricity losses from pv module soiling, degradation, and catastrophic failure.

present value, N the number of years, and I_0 the shareholder investment in the project.

In net present value analysis, the cost of capital is a predetermined value and is equivalent to the opportunity cost of capital. The cost of capital is defined as a weighted average cost of capital and includes the firm's capital structure, the cost of equity and debt capital, and tax rates. The formula for the weighted average cost of capital (WACC) is

$$\text{WACC} = \text{Discount Rate} = \{[(\%\ \text{equity})(k\ \text{equity})] \times [(\%\ \text{debt})(k\ \text{debt})(1-\tau)]\}, \quad (2)$$

where % equity is the percentage of the market value of the firm's market value owned by shareholders, k equity is the cost of equity capital, % debt is the percentage of firm's market value owned by creditors, k debt is the cost of debt, and τ is the tax rate.

Operating cash flows are revenues (Rev) minus direct costs that include variable costs (VC) and fixed cash costs (FCC):

$$\text{Operating cash flows} = \text{Rev} - \text{VC} - \text{FCC}.$$

Since net cash flows are defined as the after-tax cash flows from operations, taxes have to be included:

$$\text{Taxes on operating cash flows} = \tau(\text{Rev} - \text{VC} - \text{FCC} - \text{depreciation}).$$

Depreciation is defined as a non-cash charge against revenues in the calculation of net cash flows.

Interest expenses and their tax shield are not included in the definition of cash flows for capital budgeting purposes. The reason is that when discounting at the weighted average cost of capital, the implicit assumption is that capital budgeting projects will return the expected interest payments to creditors and the expected dividends to shareholders. Meanwhile, the reduction in expenses from the tax shield is already counted in the term for the tax rate. Hence, the inclusion of interest payments or dividends as a cash flow is double-counting. Putting all of this together, the operational expression for the calculation of the net present value (NPV) of net cash

Please cite this article as: Mason JE, Zweibel K. Baseline model of a centralized pv electrolytic hydrogen system. Int J Hydrogen Energy (2007), doi: 10.1016/j.ijhydene.2006.12.019

flows is

$$\mathrm{NPV} = \sum_{t=1}^{N}[[(\mathrm{Rev} - \mathrm{VC} - \mathrm{FCC} - \mathrm{dep})_t(1-\tau)_t]/(1+k)^t] - I_0, \quad (3)$$

which is equivalent to Eq. (1).

The levelized pv electricity and H_2 prices presented in this study are derived from Eq. (3) by selecting the price that generates a revenue level resulting in a zero net present value for the sum of net cash flow streams over the investment period.

It is assumed that the inflation rate is the same for all cash inflows, cash outflows, and rates of return. The inflation assumption implies that the inflation factor in Eq. (1) is the same in both the numerator and denominator, and hence, cancels out. Therefore, the net present value is both a nominal and real value. However, if the expected inflation rate for cash inflows, cash outflows, or rates of return are different, then inflation factors need to be added to the appropriate factors in Eq. (1) or equivalently in Eq. (3).

The discount rate for this study is 6% and is derived from the following parameters. The capital structure of firms is assumed to be 30% equity and 70% debt. The cost of equity capital is 10%, the cost of debt is 7%, and the effective income tax rate is 39%. The debt instrument is assumed to be a 20-year, 7% coupon bond.

The operating life of many H_2 system components is 60 years, and two models are used to estimate the levelized H_2 pump price. The first model estimates the levelized H_2 pump price for H_2 production and distribution in Years 1–30, which is the initial investment and debt recovery period. The second model estimates the levelized H_2 pump price for H_2 production and distribution in Years 31–60, which is the post-amortization H_2 production period.

The central financial assumption for the calculation of Years 31–60 levelized H_2 pump price is the assignment of the depreciated 10% value of Years 1–30 assets as the Years 31–60 investment value for equity holders. All other Years 31–60 capital investments, revenues, expenses, depreciation, and taxes are entered into the net present value cash flow model in exactly the same manner as the Years 1–30 model.

Sensitivity analyses are performed to evaluate the effect of change in H_2 system component parameters on levelized H_2 pump prices. The sensitivity analysis estimates are derived by the least-squares, linear regression method. The regression results provide an estimate of the effect of changes in H_2 system component values on H_2 pump prices. The regression parameters can be used to evaluate the effect of various combinations of change in the values of H_2 system components on H_2 pump prices.

3.3. H_2 compression energy calculation

The compression of H_2 for pipeline transport and local distribution uses a large quantity of energy. H_2 compression energy is estimated with the adiabatic compression energy formula

$$W_{\mathrm{J/kg}} = (y/y-1)P_1V_1[(P_2/P_1)^{(y-1)/y} - 1] \times [(Z_1+Z_2)/(2Z_1)]/\mathrm{efficiency}, \quad (4)$$

where $W_{\mathrm{J/kg}}$ is the specific compression work; y the specific heat ratio (adiabatic coefficient); P_1 the initial pressure (Pa A); P_2 the final pressure (Pa A); V_1 the initial specific volume (m^3/kg); Z_1 the gas compressibility factor for initial pressure; Z_2 the gas compressibility factor for final pressure; and efficiency the efficiency of the compressors [18]. The gas compressibility factors are calculated by the Redlich–Kwon equation of state [19]. An average compressor efficiency of 70% is assumed over the 0.8–11.72 MPa range of pressures used in this study.

The energy sources for H_2 compression points are: pv electricity for electrolysis plant and pipeline compression station compressors; pipeline H_2 for pipeline booster compressors, underground storage compressors, and city gate distribution center compressors; and grid-distributed electricity for filling station compressors.

3.4. Life cycle energy use and carbon dioxide emissions analyses

The boundaries of the life cycle energy and CO_2 emissions analyses are "cradle to grave." Five life cycle stages are evaluated: Stage 1—materials production, which includes ore extraction, milling, part casting and machining, and transportation; Stage 2—product manufacture and assembly; Stage 3—product distribution; Stage 4—product utilization; and Stage 5—product disposal. Construction, office facility utilization and employee travel to and from work are included. All components are scaled to a 30-year operating life.

A life cycle inventory is compiled for all H_2 system components with specifications provided by component manufacturers. Life cycle primary energy and CO_2 emissions parameters are then applied to the inventory items. The life cycle energy and CO_2 emissions parameters used in this study are from the following sources: pv power plant parameters are from Mason et al. [20] and Fthenakis and Alsema [21]; electrolyser, compressor, water pump, pipeline, filling station dispensers and MH container stands, and other miscellaneous component parameters are derived by the method of Weiss et al. [22] and augmented with data from Environdec Environmental Product Declarations [23]; MH parameters are from Singh [24]; building and pavement parameters are from Wibberley [25]; light duty vehicle parameters are from Weiss et al. [26]; heavy truck parameters are from Gaines et al. [27]; and fuel and electricity parameters are from GREET1.6 [28].[6] CO_2 emissions from the life cycle energy sources are estimated with GREET1.6. Recycling credits are allocated to the material production life cycle estimation parameters on the basis that 80% of materials are recycled at end-of-life.

[6] While the life cycle method used in this study is crude compared to life cycle inventory software packages, prior research has found that the results generated with the method used in this study is within 10% of the life cycle energy and CO_2 emissions results generated by life cycle software packages; 2% lower on the energy use estimate and 9% higher on the CO_2 emissions estimate [20].

Please cite this article as: Mason JE, Zweibel K. Baseline model of a centralized pv electrolytic hydrogen system. Int J Hydrogen Energy (2007), doi: 10.1016/j.ijhydene.2006.12.019

All energy values are reported in terms of MJ_{prim}/kg of H_2 consumption, where prim is primary energy. Primary energy is the total fuel cycle energy per unit of energy consumed and accounts for the energy expended to extract, refine and deliver fuels. Electricity generation is based on a US average fuel mix and power plant efficiency. Energy values are reported at their lower heating value. The CO_2 emissions estimates reported in this study are carbon dioxide, nitrous oxide and methane and are reported as kg of CO_2 equivalencies per kg of H_2 consumption. Energy and CO_2 emissions payback times are calculated to estimate the time it takes to recover the energy and CO_2 emissions embodied in the H_2 fuel cycle of H_2 powered vehicles compared to the energy and CO_2 emissions embodied in the gasoline fuel cycle of conventional vehicles. Payback time calculations are based on an average fuel economy for conventional gasoline vehicles of 10.0 km/l of gasoline and an average travel distance of 17,700 km/year/vehicle.

A generalized analysis such as this produces only approximate life cycle primary energy use and CO_2 emissions estimates because of cross-sectional variation in product and material production processes and local energy sources. Sensitivity analysis is an analytical tool to evaluate the effect of variances in life cycle estimation parameters on results. The sensitivity analysis evaluates the cumulative effect of a 25% variance in life cycle estimation parameters.

The use of major materials comprising the H_2 system is evaluated in terms of resource utilization with resource data from the US Geological Survey [29]. An important issue is the resource availability of tellurium and indium, which are critical metals in the production of thin film pv. This study conducts a "soft" analysis of potential tellurium and indium production levels with a conservative and transparent method. The objective is to evaluate whether the tellurium and indium resource bases can support the quantity of thin film pv to produce H_2 for 250-million vehicles or ~20% of the world's light-duty vehicles and light commercial trucks by 2050.

The tellurium and indium production level estimates are not intended to be definitive but to provide a general idea of what can be expected. The assumptions are: (1) current production levels of copper and zinc are maintained over time; (2) potential tellurium production is 4000 metric tons from copper mines with economically recoverable tellurium content, and potential indium production is 1600 metric tons from zinc mines with economically recoverable indium content [30]; (3) the demand for uses of tellurium and indium and tellurium other than pv will grow by 50%; and (4) the semiconductor layer thickness in the manufacture of CdTe pv is 6.5 g Te/m^2 at a 2 μm thickness and of CIGS pv is 2.9 g In/m^2 at a 1.5 μm thickness. No additional sources of tellurium or indium production are considered such as from coal residues or seabed ferromanganese crusts. Also, not considered are likely reductions in the layer thicknesses of tellurium and indium for pv module production, which will reduce tellurium and indium use.

The use of hazardous materials in the production of thin film pv is not included in this study because the issue has been thoroughly investigated in previous studies [31–33]. To date no hazardous material problems specific to the thin film pv industry have been identified. However, it is important for research to continue in this area.

4. Findings

4.1. Capital investment and levelized H_2 pump price estimates

The capital investment estimates are presented in Fig. 3. The total capital investment in the scaled pv electrolytic H_2 production and distribution system is $12.4 billion. The largest capital components are pv modules at $3.7 billion, pv power plant balance of system components at $3.1 billion, electrolysers at $2.2 billion, MH containers at $1.3 billion, and pipeline at $1.2 billion. The capital cost of the pv power plant accounts for 59% of total capital costs. With the addition of electrolysers, the total capital investment for the pv electrolysis plant is $9.5 billion or 77% of total H_2 system capital. The pipeline delivery system and city gate distribution centers are the next largest capital components with capital investments of ~$1.4 billion each and combined contribute 23% to total H_2 system capital. MH containers comprise 94% of total city gate distribution center capital. The capital for local refueling stations is $52.3 million and represents only 0.4% of total H_2 system capital investments.

The levelized H_2 pump price estimates are presented in Fig. 4. The levelized pump price of H_2 is $6.48/kg.[7] H_2 production cost is 72% of the levelized H_2 pump price. Pipeline and MH container costs contribute 15% and 10% to the levelized H_2 pump price, respectively. Total city gate distribution center costs account for 12% of the levelized H_2 pump price, and local refueling station costs account for 1%.

When the effects of individual system components are evaluated, electricity cost is found to be the single largest factor in determining H_2 pump price. The cost of electricity contributes 58% to the levelized H_2 pump price. An interesting finding is the effect of the low electrolyser utilization capacity factor on H_2 production cost. The relationship of electricity cost on the cost of electrolytic H_2 production across the range of electrolyser utilization capacity factors is presented in Fig. 5. Comparing levelized H_2 production cost with a 25% electrolyser capacity factor to a 95% electrolyser capacity factor, the H_2 production cost is only 11% higher in the low capacity factor case.[8] The H_2 production cost penalty of the low electrolyser

[7] To provide perspective to the H_2 pump price, the gasoline equivalent price is $0.74/l gasoline equivalent ($2.79/gallon gasoline equivalent). The assumptions for the calculation of the H_2 gasoline equivalent price are an average fuel economy of H_2 powered vehicles of 87.6 km/kg of H_2 and an average fuel economy of conventional gasoline powered vehicles of 10.0 km/l of gasoline.

[8] From Fig. 3, it is obvious that the relationship between electrolyser cost and H_2 production cost across a 25–95% capacity factor range is non-linear. In this case, the appropriate method to evaluate the effect of electrolyser cost on H_2 production cost across the range of electrolyser capacity factors is a log-linear regression model. A log-linear regression model transforms the non-linear dependent variable, H_2 production cost, into a linear variable by using its natural logarithm value. The log-linear regression result indicates that a 1% increase in electrolyser capacity factor reduces H_2 production cost by 0.16%. Hence, a 70% increase in electrolyser capacity factor decreases H_2 production cost by only 11.2% (0.16% × 70).

Please cite this article as: Mason JE, Zweibel K. Baseline model of a centralized pv electrolytic hydrogen system. Int J Hydrogen Energy (2007), doi: 10.1016/j.ijhydene.2006.12.019

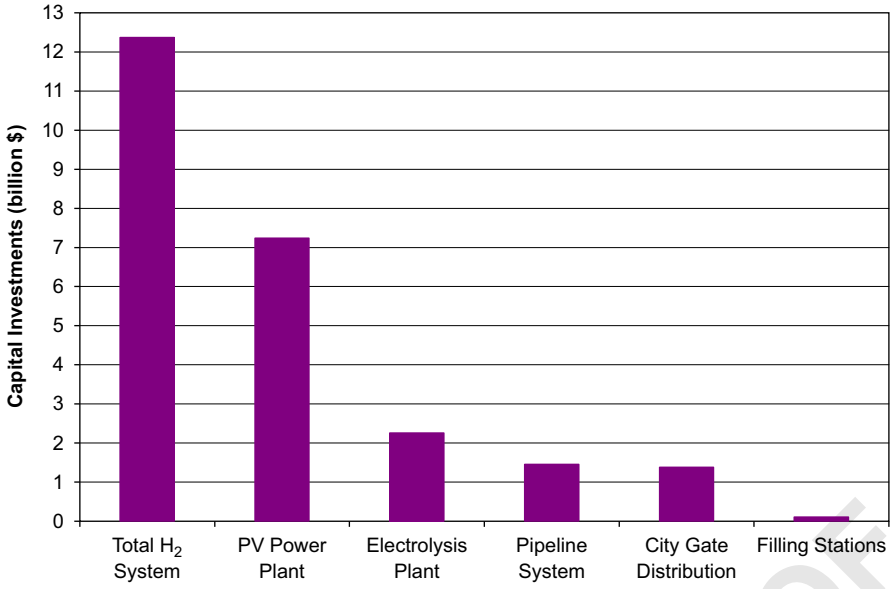

Fig. 3. Capital investments.

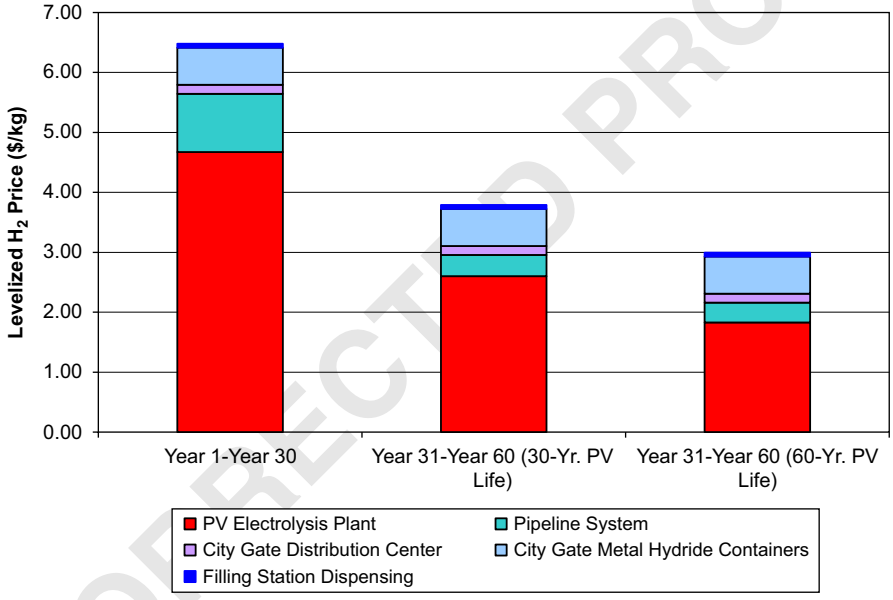

Fig. 4. Levelized H_2 pump prices.

utilization factor is moderated by the 50% reduction in annual electrolyser O&M expense.

A most important finding is the 45–54% reduction in H_2 pump price for the post-amortization, Years 31–60, H_2 production period. If pv modules have to be replaced after 30 years, which is the standard assumption of conventional pv analysis, then the H_2 pump price reduction in Years 31–60 is 45% to $3.79/kg. However, if the operating life of pv modules is 60 years with an average 1% annual pv electricity output degradation rate, then the levelized H_2 pump price reduction is 54% to $3.00/kg for Years 31–60 H_2 production (Figs. 6–8).

Sensitivity analysis is performed to evaluate the effect of changes in the cost and performance parameters of H_2 system components on levelized H_2 pump price. The descriptive statistics in Table 2 present the range of values used to generate the regression results of the sensitivity analysis. The sensitivity findings are presented in Table 3. As previously noted, change in electricity cost has a large effect on H_2 pump price. A $0.01/kW h decrease in electricity cost decreases the H_2 pump price by $0.56/kg. One of the best means to reduce pv electricity cost is with an increase in pv module efficiency while holding pv module production cost constant. A 1% increase in pv module efficiency, for example from 10% to 11%, decreases the H_2 pump price by $0.24/kg. This finding is important because an increase in the efficiency of pv modules above the 10% baseline model of this study is highly probable.

The regression results presented in Table 3 can be used as a general template to evaluate the effect on H_2 pump prices

Please cite this article as: Mason JE, Zweibel K. Baseline model of a centralized pv electrolytic hydrogen system. Int J Hydrogen Energy (2007), doi: 10.1016/j.ijhydene.2006.12.019

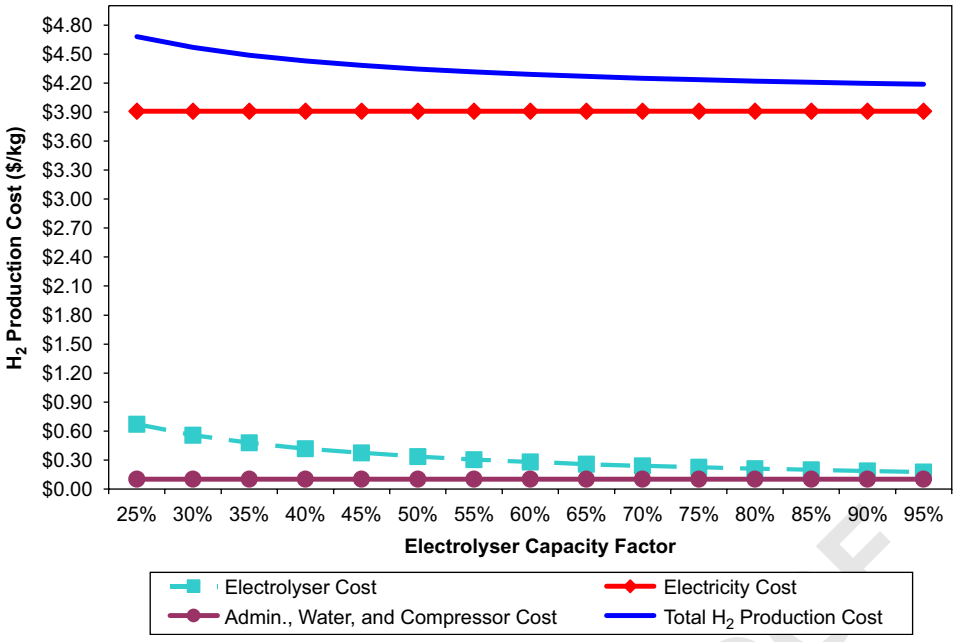

Fig. 5. Levelized H_2 production price as a function of electrolyser capacity utilization.

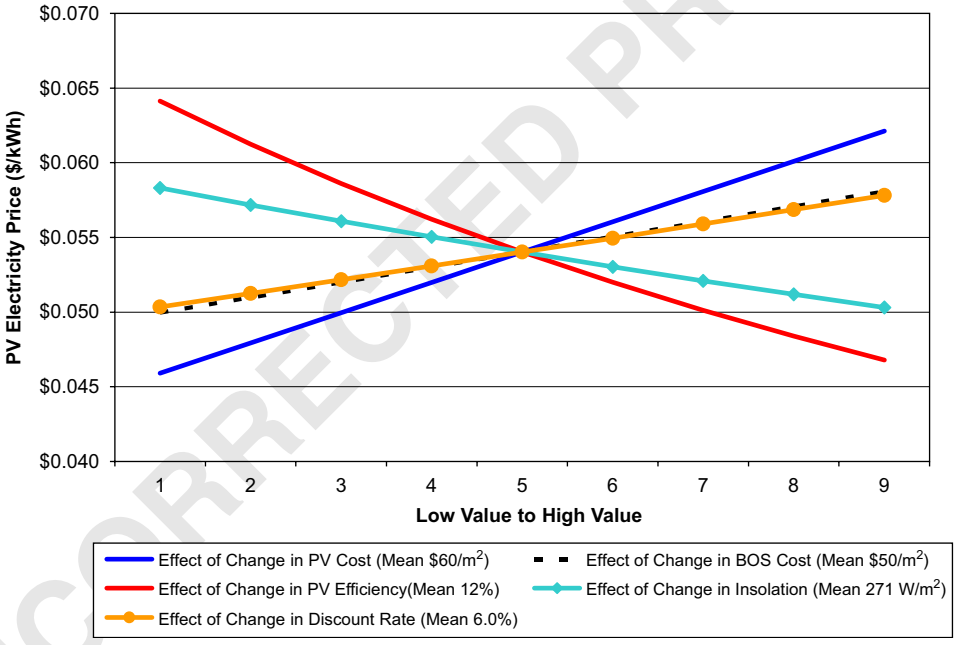

Fig. 6. Sensitivity of pv electricity price to change in factor values.

caused by various changes in the levels and combinations of H_2 system component values. For example, if pv module efficiency increases by 2%, pv BOS cost is reduced by \$5/m^2, and the cost of MH containers is reduced by \$5/kg, then the H_2 pump price is reduced by \$0.70/kg H_2 or 10%.

4.2. Life cycle energy use and CO_2 emissions

The life cycle energy use and CO_2 emissions findings are presented in Table 4. The total primary energy embodied in the life cycle of the pv electrolytic H_2 production and distribution system is 36 MJ/kg of H_2 consumption. Of the total life cycle energy, the pv electrolysis plant accounts for 64%, filling stations account for 33%, and the pipeline and city gate distribution account for less than 2% each. The total life cycle CO_2 emissions are 2.6 kg CO_2 Eq/kg of H_2 consumption. The high primary energy use and CO_2 emissions of filling stations is attributable to the use of grid-distributed electricity as the power source for filling station compressors. The other compression points in the H_2 distribution system are using either pv electric-

Please cite this article as: Mason JE, Zweibel K. Baseline model of a centralized pv electrolytic hydrogen system. Int J Hydrogen Energy (2007), doi: 10.1016/j.ijhydene.2006.12.019

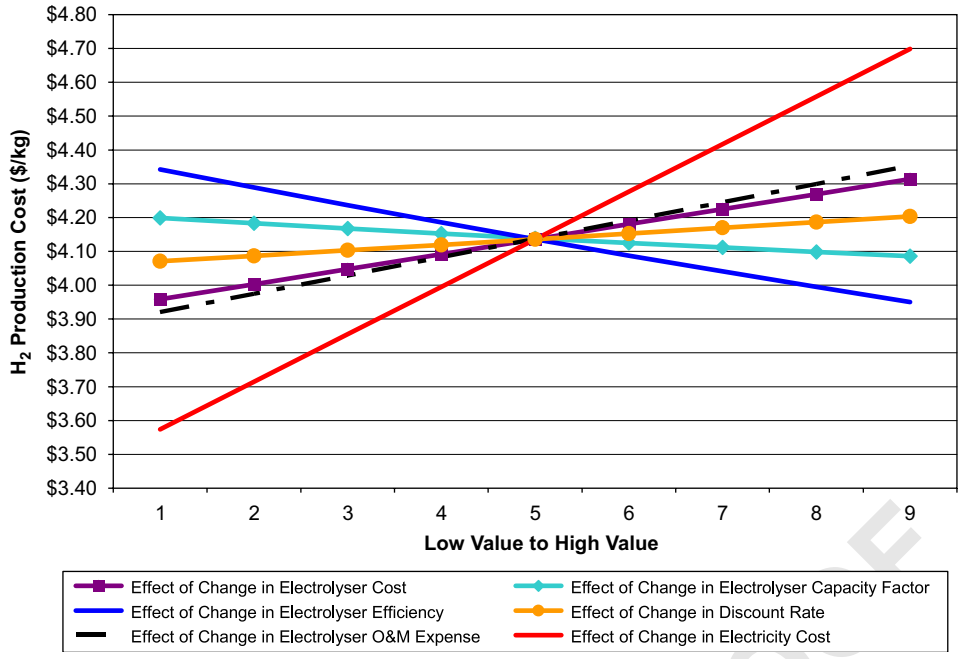

Fig. 7. Sensitivity of H_2 production cost to change in factor values.

ity or H_2 to power the compressors, which have significantly lower life cycle energy use and CO_2 emissions.

The energy and CO_2 emissions payback times and sensitivity results are presented in Table 6. The primary energy payback time is 3.1 years, and the CO_2 emissions payback time is 3.1 years. With a 30-year life cycle for all system components, the payback times translates into 27 years of fossil fuel energy free and zero CO_2 emissions vehicle operation with the replacement of gasoline powered vehicles with H_2 powered vehicles. The sensitivity results indicate that a ±25% change in all life cycle estimation parameters change the primary energy and CO_2 emissions payback times by ±0.8 years.

Another way to assess the life cycle energy use and CO_2 emissions is to compare the annual fuel cycle totals of H_2 powered vehicles to the annual fuel cycle totals of gasoline powered vehicles. The annual primary energy consumption and CO_2 emissions from the fuel cycle of one million H_2 powered vehicles is 90% less than those of one million conventional gasoline powered vehicles. This comparison can be extended by including life cycle energy and CO_2 emissions embodied in the manufacture of FCV and conventional gasoline internal combustion engine vehicles. Research indicates that the life cycle energy and CO_2 emissions embodied in the manufacture of FCV is basically the same as those embodied in the manufacture of current conventional gasoline vehicles [26]. This finding lends support to the conclusion that pv electrolytic H_2 powered vehicles reduce primary energy use and CO_2 emissions by 90%. The CO_2 emissions reduction of H_2 systems will increase over time as solar, wind, and H_2 energy sources comprise an ever greater proportion of the energy mix used in the manufacturing and distribution phases of H_2 system components.

4.3. Energy consumption for H_2 compression

The total energy to compress H_2 for pipeline transport, local distribution and vehicle refueling is 3932 TJ, which is 13% of the energy value of gross H_2 production. The compression energy estimates for each of the compression points are presented in Table 5. The actual quantity of primary energy consumed is much less since the energy for pipeline and city gate compression is provided by pv and H_2.

The total primary energy use for all compression points is 1178 TJ, which is 4% of the energy value of gross H_2 production. While the electrolysis plant and pipeline compression use the most energy, 72% of total compression energy use, their contribution to primary energy consumption is just 32% because of the use of pv electricity and H_2 to power the compressors. The use of grid-distributed electricity for filling station compressors is the weak point in the system in terms of primary energy use and CO_2 emissions. While the energy for filling station compressors is only 18% of total compression energy, the contribution to total primary energy is 61%. The installation of pv at filling stations to help power the compressions could significantly reduce primary energy consumption and CO_2 emissions.

4.4. Resource utilization

4.4.1. Materials

The impact of a pv electrolytic H_2 production and distribution system on material resources is presented in Table 6. The quantity of steel, aluminum and copper required for the H_2 system is relatively insignificant in relation to the annual production levels of these resources. However, the supply of rare

Please cite this article as: Mason JE, Zweibel K. Baseline model of a centralized pv electrolytic hydrogen system. Int J Hydrogen Energy (2007), doi: 10.1016/j.ijhydene.2006.12.019

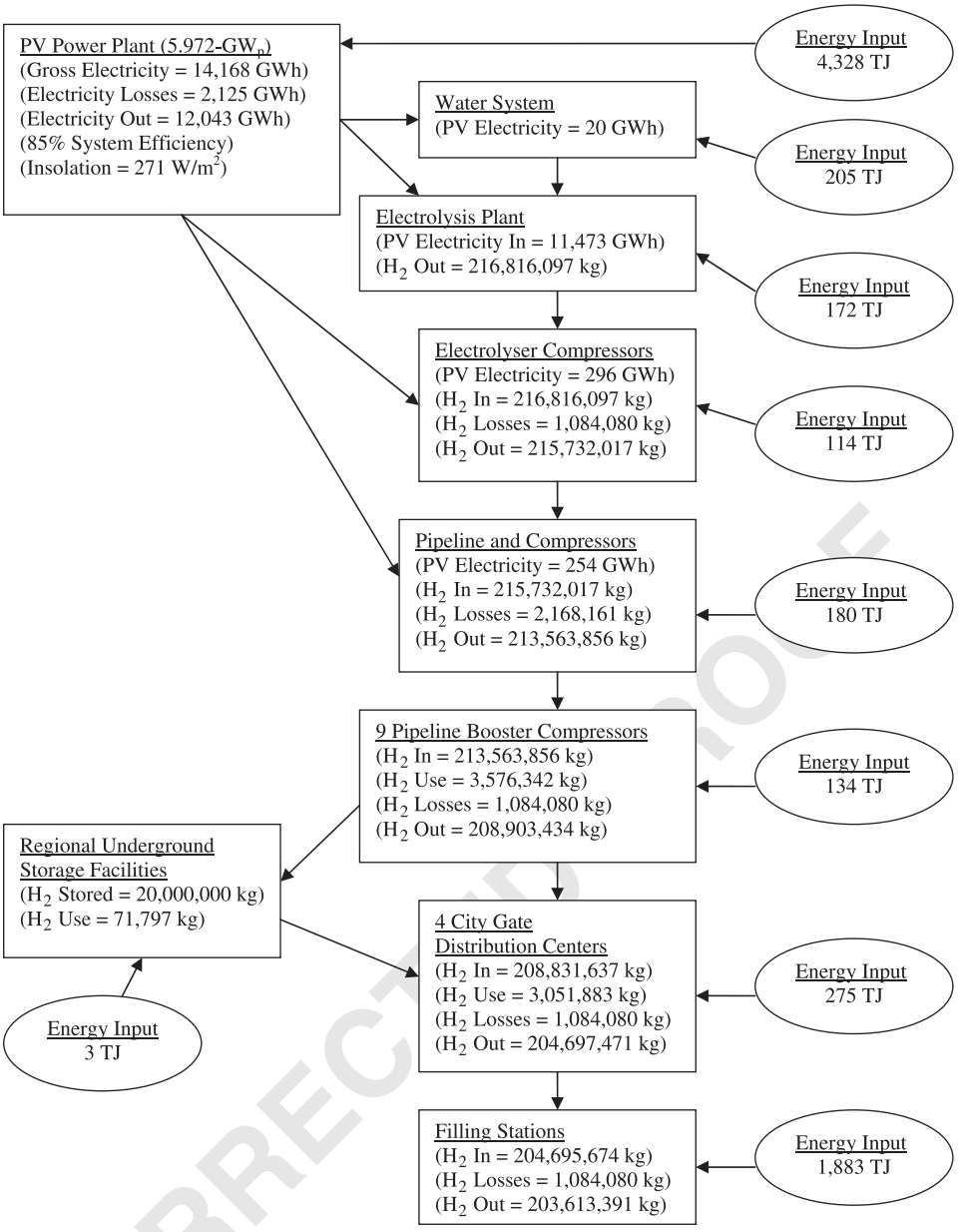

Fig. 8. H_2 system energy flow chart (lower heating values). *Notes*: Energy inputs in the right column are primary energy estimates for the system components.

semiconductor metals used in the manufacture of thin film pv technologies raises resource availability issues. It is obvious from the data in Table 6 that the annual production of the rare semiconductor metals tellurium and indium must be increased to support growth in the manufacturing capacity of thin film CdTe and CIS pv technologies, respectively.

Tellurium in CdTe pv and indium in CIS pv are the least abundant materials in thin film pv manufacture. These metals are not mined directly but are extracted from the concentrates and residues of primary metal production such as copper and zinc. At present, tellurium and indium are extracted from only a small percentage of the primary ore concentrates and residues that contain these metals. The capital cost to add secondary metal processing units at metal smelters is $3–$5 million. Large increases in thin film pv production will require the coordination of expanding tellurium and indium production. The timely increase in the supply of the metals is more important than the actual price of the metal itself since the semiconductor component is less than 5% of the total manufacturing costs of thin film pv [34]. It should be noted that the exact resource levels of tellurium and indium is debatable, which clouds the assessment of the high-end of annual thin film pv production levels.

Estimates of the quantity of pv required to produce a supply of H_2 to support 250-million H_2 powered vehicles are presented in Table 7. If the pv electrolytic implementation period is 30 years, then eight 6.0-GW_p pv power plants will have to be built annually. With pv additions for degradation losses, the annual pv manufacturing capacity is 50-GW_p. This raises the issue of tellurium and indium resource availability. From the

Please cite this article as: Mason JE, Zweibel K. Baseline model of a centralized pv electrolytic hydrogen system. Int J Hydrogen Energy (2007), doi: 10.1016/j.ijhydene.2006.12.019

Table 2
Sensitivity of levelized H_2 pump price to change in component cost

(A) Effect of change in electrolysis plant values	Change in H_2 pump price (¢/kg H_2)[a]
Electrolysis plant	
Electricity cost (per ¢/kW h)	56.2
Electrolyser cost (per \$25/$kW_{dc\text{-}in}$)	4.4
Electrolyser capacity factor (per 1.0%)	−2.9
Electrolyser efficiency (per 1.0%)	−4.9
Electrolyser O&M expense (per 0.5%)	5.3
Electrolysis plant discount rate (per 0.5%)	4.2
(B) Effect of change in H_2 distribution values	
Pipeline (per \$250,000/mile)	7.7
Metal hydride containers (per \$5/kg)	9.9
(C) Effect of change in pv power plant values on pv electricity price	Change in PV electricity price (¢/kW h)
pv cost \$/m^2 (per \$5/m^2)	0.2
BOS cost \$/m^2 (per \$5/m^2)	0.2
pv efficiency (per 1.0%)	−0.4
Insolation level (per 0.5 kW h/day)	−0.6
Land lease (per \$2500/ha)	0.05
Discount rate (per 0.5%)	0.2

[a]A negative sign in the results column indicates a negative relationship, which means that the stated unit increase in the component value (the value in parenthesis) leads to a decrease in the H_2 pump price, and a unit decrease in the component value leads to an increase in the H_2 pump price.

Table 3
Energy and CO_2 emissions payback time and sensitivity analysis

System components	Primary energy (MJ_{prim}/kg H_2)	CO_2 Eq emissions (kg CO_2/kg H_2)	Payback sensitivity of energy to plus/minus 25% (years)	Payback sensitivity of GHG emissions plus/minus 25% (years)
pv power plant	21.26	1.5	0.48	0.47
Water system	1.01	0.1	0.02	0.02
Electrolysis plant	1.40	0.1	0.03	0.03
Pipeline	1.56	0.1	0.03	0.04
City gate distribution	1.35	0.1	0.03	0.03
Filling stations	9.25	0.7	0.21	0.22
Totals	35.82	2.6	0.80	0.81
Payback time (years)	3.1	3.1		
Reduction (%)	89.7	89.7		

Notes: a. Life cycle results are based on annual H_2 consumption of 203,613,391 kg H_2.
b. The H_2 system payback times and % reductions are derived from the operation of one-million conventional ICE vehicles with a fuel economy of 10 km/l gasoline. The primary energy value of gasoline is 40 MJ_{prim}/l (LHV), and gasoline combustion carbon dioxide equivalent emissions are 2.86 kg CO_2 Eq per liter gasoline [26].

results in Table 6, potential production levels of tellurium and indium from current levels of copper and zinc production are sufficient to support 50-GW_p/year of thin film pv production. It should be noted that the production levels presented in Table 6 do not include all sources of tellurium and indium production or reduction in layer thickness for pv module manufacture. Theoretical considerations suggest that the amounts could be as low as 1.6 g/m^2 for tellurium and 1 g/m^2 for indium in 0.5 μm thick cells, while still maintaining high efficiencies. With these reductions in the quantity of tellurium and indium, pv production levels can be a factor of four greater for CdTe pv and a factor of three greater for CIGS pv. Most importantly a very large source of economically recoverable tellurium has recently been discovered in seabed ferromanganese crusts [35].

While ocean floor mining today is in its infancy, over the next several decades ocean floor mining will likely grow in importance to sustain growth in primary and secondary metal production levels to support global industrial growth. Therefore, the long-term supply of tellurium is believed sufficient to support any conceivable level of CdTe pv production over the course of the 21st Century. And the application of cadmium in pv modules safely removes that amount of cadmium from having to be disposed of in other potentially harmful or costly ways.

The primary challenges for pv development are: continued progress in thin film pv module efficiencies and cost reduction; the scale-up in the manufacturing capacity of pv and electrolyser components; and increasing the production of tellurium

Please cite this article as: Mason JE, Zweibel K. Baseline model of a centralized pv electrolytic hydrogen system. Int J Hydrogen Energy (2007), doi: 10.1016/j.ijhydene.2006.12.019

Table 4
Compression energy for H_2 pipeline transport, city gate distribution, and filling station vehicle H_2 dispensing

Compression points	Begin pressure (MPa)	Final pressure (MPa)	Compression energy (kW h/kg)	H_2 energy (%)
Electrolysis plant	0.10	0.80	1.37	3.5
Pipeline compression station	0.69	6.89	1.25	3.2
Pipeline booster compression (9)	5.50	6.89	1.08	2.7
City gate compression	5.50	12.00	0.43	1.1
Filling station compression	2.50	12.00	0.98	2.5
Total compression energy			5.12	13.0
Compression points		H_2 flow (kg/yr)	Compression energy (TJ)	Compression primary energy (TJ)[a]
Electrolysis plant		216,816,097	1069	107
Pipeline compression station		215,732,017	971	97
Pipeline booster compression points (9)		213,563,856	830	249
City gate compression		208,831,637	323	97
Filling station compression		204,695,674	722	2137
Total compression energy			3932	2687

[a]The primary energy for pv electricity consumption is 0.1 MJ_{prim}/MJ of pv electricity, and the primary energy for H_2 consumption is 0.3 MJ_{prim}/MJ of H_2. The pv electricity and H_2 primary energy estimates are based on the findings of this study. The energy content of H_2 is 120 MJ/kg at the low heating value. The primary energy for grid-distributed electricity is 2.96 MJ_{prim}/MJ of wall-outlet electricity, which is based on US average fuel and power plant mix [26].

Table 5
Resource utilization and availability for pv electrolytic H_2 systems

(metric ton)	Current world production (2005)[a] (t)	Current potential world production[b] (t)	6.034-GW_p/yr pv electrolytic H_2 production and distribution system (t)	Current world production (%)
Steel	850		536,059	0.1
Aluminum	26		9218	0.0
Copper	15		36,495	0.3
PV least common material				Annual pv production potential (GW_p)
(1) CdTe PV (10% efficiency)				
Tellurium	130	4000		
2.0 μm thick cells @ 6.5 g Te/m^2			392	58
0.5 μm thick cells @ 1.6 g Te/m^2			97	237
(2) CIGS PV (10% efficiency)				
Indium	455	1600		
1.5 μm thick cells @ 2.9 g In/m^2			175	31
0.5 μm thick cells @ 1.0 g In/m^2			61	91

[a]The US Geological Survey's Annual Mineral Commodity Summaries are the source for 2005 world metal production estimates. It is assumed that all current world production of tellurium and indium is for uses other than pv.
[b]The data source for current potential world production of tellurium and indium is Sanden [28]. Copper is the primary ore source for tellurium production, and zinc is the primary ore source for indium production.

and indium. To hedge against the remote possibility that the supply of tellurium and indium falls short, further research on silicon based pv as well as new compound semiconductor thin films is important. Since the future supply of tellurium and indium is unpredictable in an absolute sense, this research emphasis in pv is a necessary component of any strategy for the terawatt-scale application of pv. Recycling processes for the full recovery of metals from retired pv modules will also extend the long-term supply of rare semiconductor metals.

4.4.2. Land

The land area of the pv electrolysis plant is a function of pv module efficiency, the spacing between the rows of the pv arrays, and the land required for electrolysers, compressors and water storage, pumping and distillation. The assumed pv module efficiency is 10.0%, which is 100 W_p/m^2. The area of the pv plant is a factor of three greater than the area of pv modules to provide adequate spacing between array rows to prevent module cross-shading from 9:00 am to 4:00 pm on De-

Please cite this article as: Mason JE, Zweibel K. Baseline model of a centralized pv electrolytic hydrogen system. Int J Hydrogen Energy (2007), doi: 10.1016/j.ijhydene.2006.12.019

Table 6
Installed pv and capital costs to produce H_2 for 250-million FCVs with the 30-year lifetime scenario and first generation assumptions

	New pv installed/year (GW_p)	Total pv installed in 30 years (GW_p)	Number of pv manufacturing plants @ 3-GW_p/year capacity
pv electrolysis plants[a]	49.76	1493	17.6
pv additions for output losses[b]	0.52	242	0.2
Total installed pv	50.28	1735	23.0
	H_2 system with 10% efficient pv	H_2 system with 12% efficient pv	H_2 system with 14% efficient pv
Annual capital costs (billion $)	95.1	85.7	78.9
Total 30-year capital costs (billion $)	2853	2570	2367

[a]Includes pv for electrolysers, compressors, water pumps, water distillation, and the pipeline compression station. Each year 8.3, 6.034-GW_p pv power plants will need to be constructed.

[b]The pv additions for the 49.6 GW_p of pv installed in the first year are 0.52 GW_p per year for 30 years. The pv additions increase each year by 0.52 GW_p. In the 13th year, the total quantity of pv additions is 15.73 GW_p. Hence, the pv manufacturing capacity of five additional 3-GW_p/year pv manufacturing plants will be needed to supply the pv additions. A total of 23 pv manufacturing plants with an annual production capacity of 3-GW_p will need to be in production in year 30.

Table 7
2007–2020 capital cost estimates for a pv powered distributed electrolysis plant

		2007	2010	2020
(*A*) *Central pv power plant*[a]				
pv modules	($/m^2)	150	100	60
BOS components	($/m^2)	65	60	50
DC–AC inverters	($kW_{dc\text{-}in}$)	45	40	25
(*B*) 265-$MW_{el\text{-}in}$ *distributed electrolysis plant*[b]				
Electrolysis plant	($/$kW_{el\text{-}in}$)	850	765	550

[a]The pv power plant capital cost estimates for 2007 are speculative because of confidentiality. The estimates are believed reasonable based on our research of current state-of-the-art thin film multi-MW_p pv power plants.

[b]The 2007 price estimate for the 265-$MW_{el\text{-}in}$ distributed electrolysis plant is from Norsk Hydro and stated in 2007 US dollars. The 2010 and 2020 reductions assume a 10% reduction in 2010 with the construction of one plant per year and a 33% reduction in 2020 with the construction of two plants per year. The components include plant construction, electrolysers, transformer, thyristor, lye tank feed water demineralizer, hydrogen scrubber, deoxidizer, gas holder, and compressors.

cember 21.[9] The land area for a 7.86-GW_p pv plant, which is the total quantity of pv installed over 30 years and includes the pv additions to maintain a constant level of electricity output, is 243 km^2. With electrolyser building, administration and maintenance buildings, and water system components, the total land area of the pv electrolysis plant is approximately 260 km^2. While the land area for one pv electrolysis plant is readily available, the land area to produce H_2 for 250 μm vehicles is 65,000 km^2, which is a land area that is comparable to 25% of the land area of Arizona, USA.

The large land area required for super-large-scale pv electrolytic H_2 calls into question whether or not it is appropriate in terms of CO_2 emissions reduction to use the land for H_2 production rather than pv electricity production. The National Renewable Energy Laboratory (NREL) of the US Department of Energy is conducting land availability analyses for pv and concentrating solar power (CSP) plants in the Southwest US. The NREL land assessment takes into account land use, environmentally sensitive areas, land contour, and insolation. From the information provided in the NREL map in Fig. 9, it is plausible to assume that 400,000 km^2 of land is available for pv and CSP plants in the Southwest US. This land area is sufficient to support 15,500 400-GW_e CSP power plants and 4.6-TW_p pv power plants, which is ample energy to meet projected US electricity and H_2 demand through 2100. Hence, it is reasonable to conclude that centralized pv power plants can be applied to both H_2 production for transportation and electricity production.

The US is not unique in having large desert regions with high insolation levels. China, Africa, Middle East, India, Mexico, Australia, and Argentina have large solar resources. It should also be kept in mind that pv electrolytic H_2 production requires less land area than electricity generating plants using other energy sources when mining and water are taken into account. The use of sparsely populated desert regions eliminates competition over competing land uses such as agriculture, forestry, grazing, mining, or other commercial land uses.

[9] The row spacing estimate is based on 33° latitude and a sun altitude of 14.9° above the horizon at 9:00 am. The actual row spacing is a factor of 2.88 greater than the length of the modules and 0.12 is added as a safety buffer.

Please cite this article as: Mason JE, Zweibel K. Baseline model of a centralized pv electrolytic hydrogen system. Int J Hydrogen Energy (2007), doi: 10.1016/j.ijhydene.2006.12.019

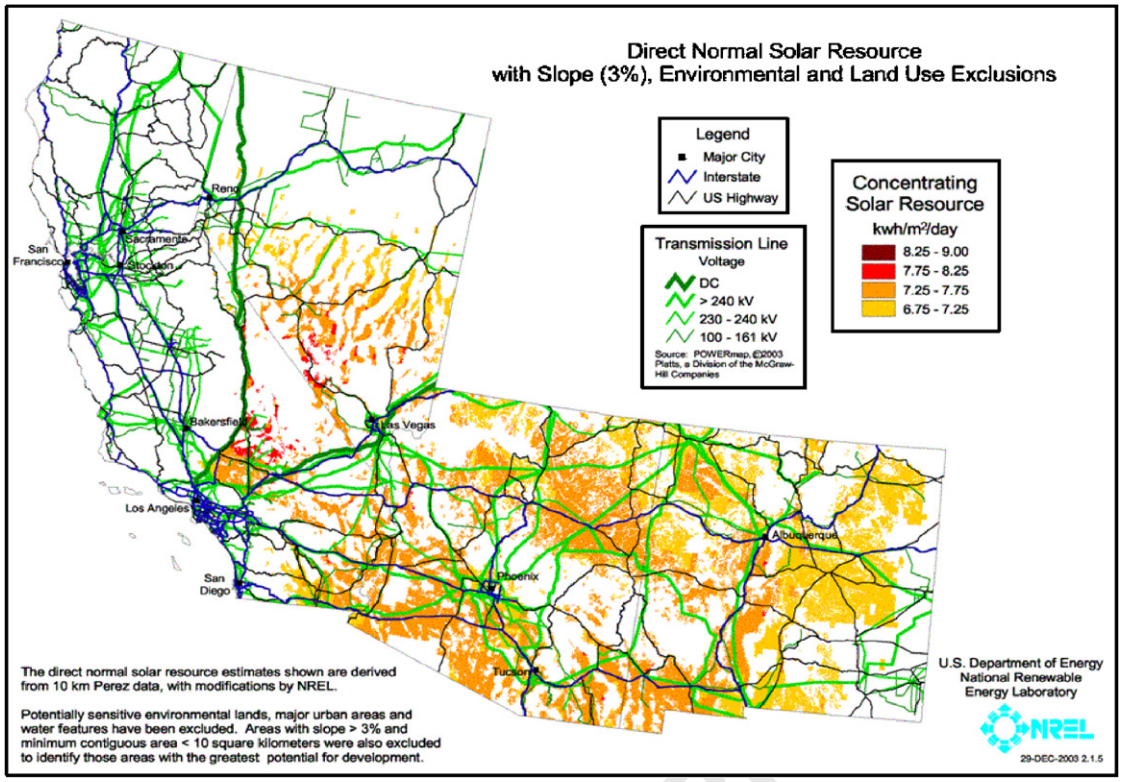

Fig. 9. Potential US land area for pv power plants.

4.4.3. Water

A water supply is required for electrolytic H_2 production and to cool electrolyser cells and compressors. The electrolysis plant and pipeline compression station require feedstock water of 11 l/kg H_2, electrolyser cell cooling water of 300 l/kg H_2, and compressor cooling water of 50 l/kg H_2 . It is assumed that electrolysis plant and compressor station have an integrated, closed-cycle water system with cooling towers. Cooling tower water losses are assumed to be 5% per hour, which includes blow-down water losses [36]. Total water consumption for the electrolysis plant and pipeline compression station is 6.8-million m^3 of water per year.[10] For super-large-scale H_2 production, this is a large quantity of water for arid regions.

Water can be supplied from several sources. The water can be supplied by an on-site water collection and storage system, desalinated water imported by train or truck, and CSP plants located in proximity to oceans can cogenerate desalinated water and electricity.[11] For a location receiving a meager 10 cm of annual rainfall, the water consumption of the pv electrolysis plant and pipeline compression station is ~10% of the rainfall on the land area of the pv plant. Under no circumstances should water be drawn from underground aquifers to support electrolytic H_2 production. The application of CSP steam power plants for seawater desalination is an exciting attribute of CSP plants in water scarce regions. The use of desalinated water, costing \$0.44/m^3, by electrolysis plants increases the price of H_2 by only \$0.005/kg compared to the use of water collected from rain-runoff.

5. Distributed electrolysis plants

This section investigates the displacement of pipeline H_2 distribution through the deployment of two types distributed electrolysis plants—distributed pv electrolysis plants and distributed electrolysis plants using pv electricity imported over power lines from high insolation regions. The two types of distributed electrolysis plants are to be located in proximity to urban H_2 markets and eliminate the requirement for a long-distance pipeline distribution network. In addition to using pv electricity, distributed electrolysis plants can use local grid electricity to increase the operating capacity factor. A comparative analysis is performed to assess the advantages and disadvantages of distributed electrolysis plants in relation to centralized pv electrolysis plants with pipeline H_2 distribution.

The technical specifications for the distributed electrolysis plant model are derived from the design of a 265-$MW_{el\text{-}in}$ elec-

[10] To put the quantity of water into perspective, a typical 90-acre golf course in Phoenix, Arizona, USA consumes 475,000 m^3 of water per year. The pv electrolyser plant water use is equivalent to 14 Phoenix golf courses [37].

[11] CSP steam power plants can be designed with back-pressure turbines to produce steam which can be transformed into water with multi-stage evaporators and 12% loss in power output. A 1-GW_e steam power plant operating 6500 h per year can produce ~150-million m^3 of desalinated water at a cost \$0.44/m^3. This quantity of desalinated water is sufficient for the steam power plant and 10 pv electrolysis plants scaled to the size of this analysis [37].

Please cite this article as: Mason JE, Zweibel K. Baseline model of a centralized pv electrolytic hydrogen system. Int J Hydrogen Energy (2007), doi: 10.1016/j.ijhydene.2006.12.019

trolysis plant by Norsk Hydro and Electricité de France [7]. The plant produces 4200 kg of H_2 per hour of operation, which is sufficient to support the operation of 50,000–175,000 H_2 vehicles over the range of capacity factors assumed in this analysis. Variation in the operating capacity factors of distributed electrolysis plant is modeled to accommodate the comparative evaluation of four plausible scenarios of pv and grid electricity supply. The four scenarios of electricity supply are (1) the sole use of pv electricity; (2) a mix of pv electricity and 8.0 h of off-peak period grid electricity; (3) a mix of pv electricity, 8.0 h of off-peak period grid electricity, and 9.5 h of intermediate and peak period grid electricity; and (4) sole use of grid electricity. The maximum operating capacity factor for electrolysis plants is assumed to be 84%, which is based on 94% plant availability during scheduled operating periods, the scheduling of 14 days per year of plant down-time for maintenance, and reservation of 20 days per year of plant down-time to free electricity supply to meet summer peak electricity demand periods.

Distributed pv electrolysis plants are evaluated first, and then distributed electrolysis plants using imported pv electricity from high insolation regions are evaluated. The advantages of distributed pv electrolysis plants are elimination of pipeline costs, an increase in the operating capacity factor of electrolysis plants due to an ability to supplement the supply of pv electricity with off-peak grid electricity, and a decrease in average electricity cost due to the low-cost of off-peak grid electricity. The primary disadvantage of distributed pv electrolysis plants is reduced pv electricity production levels, which is attributable to lower insolation levels. In addition, a decrease in insolation level increases the levelized cost of pv electricity and reduces the operating capacity factor of electrolysis plants. Another disadvantage is CO_2 emissions from the use of grid electricity.

The preclusion of pipeline costs and an increase in electrolysis plant capacity factor decreases the levelized pump price of H_2 produced by distributed electrolysis plants. The elimination of pipeline costs reduces the levelized pump price of H_2 by \$0.97/kg. And from Table 2, each percentage increase in electrolyser capacity factor decreases the levelized pump price of H_2 by \$0.029/kg. An evaluation of the effect of increased capacity factor is complicated by the range of insolation levels for possible locations of distributed electrolysis plants. The pv portion of distributed electrolysis plant capacity factor is 26%, 24%, 22%, and 20% for plant locations with average insolation levels of 6.5, 6.0, 5.5, and 5.0 kW h/m^2/day, respectively. The use of 8 h of off-peak grid electricity increases the capacity factor by 32%, and the addition of 9.5 h of intermediate and peak period grid electricity increases the capacity factor by an additional 26–32%. With the use of 8 h per day of off-peak grid electricity, the plant capacity factors are 52–58% over the above specified range of insolation levels. With the combined use of 8 h per day of off-peak grid electricity and 9.5 h of intermediate and peak period grid electricity, the plant capacity factor is 84%, which is the assumed maximum capacity factor as previously stated.

A weighted average of pv and grid electricity prices are used to estimate the net effect of electricity cost on levelized H_2 pump prices for the four electricity source scenarios. Grid electricity is evaluated at the US average fuel mix, and the average price of off-peak grid electricity is assumed to be \$0.03/kW h, and the average price for intermediate and peak period grid electricity is assumed to be \$0.08/kW h [38]. The pv electricity prices are \$0.064/kW h, \$0.070/kW h, \$0.076/kW h, and \$0.082/kW h for distributed pv power plants at locations with average daily insolation levels of 6.5, 6.0, 5.5, and 5.0 kW h/m^2/day, respectively. From Table 2, a one cent increase (decrease) in electricity cost increases (decreases) the levelized H_2 pump price by \$0.562/kg. A final factor taken into account is land cost. It is assumed that land values are a factor of 10 greater for distributed pv electrolysis plants, which means that land costs increase from \$2500/ha to \$25,000/ha.

The levelized H_2 pump price estimates for the distributed pv electrolysis plant models are presented in Fig. 10. The levelized H_2 pump prices are only slightly higher than those for the baseline centralized pv electrolysis plant model. When low-cost off-peak grid electricity is used, the levelized H_2 pump price falls sharply due to the significantly lower cost of off-peak grid electricity relative to the cost of distributed pv electricity. The cost of off-peak grid electricity is 57–63% less than the \$0.070–0.082/kW h cost of distributed pv electricity. A penalty for the use of grid electricity is an increase in fuel cycle CO_2 emissions. For an off-peak model with low CO_2 emissions, 4 h of off-peak wind electricity is incorporated at a levelized cost of \$0.086/kW h. The levelized H_2 pump price for the off-peak wind model is only 5% greater than the baseline centralized pv electrolysis plant model. In conclusion, the deployment of distributed pv electrolysis plants to displace H_2 pipelines results in only slightly higher H_2 pump price compared to the baseline pv electrolytic H_2 model with pipeline distribution.

However, a caveat must be considered. The structural specification of pv power plants is designed to withstand 193 km/h sustained winds. The structural design of pv power plants does not include concrete foundations for pv mounting frames, which calls into question the structural integrity of the pv plants in tornado climate regimes. Therefore, the deployment of pv power plants with the structural design of this analysis are likely to be limited to locations with a low probability for the occurrence of tornado events. The inclusion of concrete foundations for the pv mounting structures will increase BOS costs, which in turn will increase the levelized H_2 pump price. The estimation of BOS costs for pv mounting structures with concrete foundations is beyond the scope of this analysis.

We now examine the case of distributed electrolysis plants, which use pv electricity imported over power lines from high insolation regions. The advantages of distributed electrolysis plants are a reduction in pipeline costs, an increase in the operating capacity factor of electrolysis plants due to an ability to supplement the supply of pv electricity with off-peak grid electricity, a decrease in average electricity cost due to use of low-cost off-peak grid electricity. The disadvantage is higher pv electricity costs caused by electricity losses from an additional electricity power conditioning step, power line transmission electricity losses, power line transmission fees, and local electricity distribution fees. Another disadvantage is the CO_2 emissions from the use of grid electricity.

Please cite this article as: Mason JE, Zweibel K. Baseline model of a centralized pv electrolytic hydrogen system. Int J Hydrogen Energy (2007), doi: 10.1016/j.ijhydene.2006.12.019

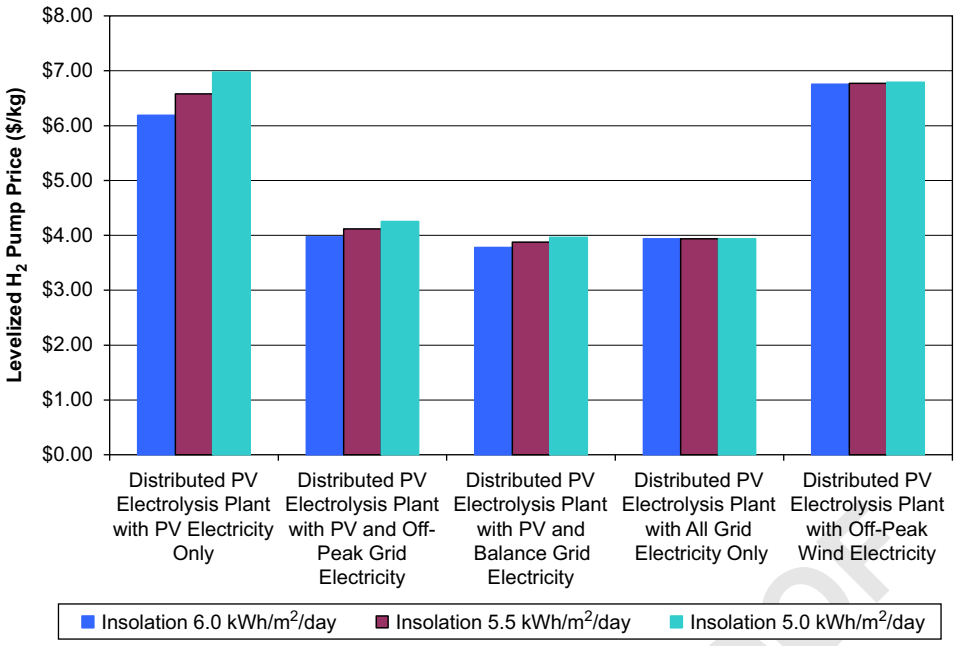

Fig. 10. Levelized H_2 pump prices for distributed pv electrolysis plants with variation in insolation levels and distributed electrolyser plant electricity sources.

The levelized imported pv electricity cost includes long-distance electricity transmission losses of 10%, long-distance power line transmission fees of $0.003/kW h, and local distribution fees of $0.015/kW h.[12] The $0.015/kW h local distribution fee for pv electricity is 50% less than the EIA $0.03/kW h cost contribution for utility administration and profits. The reduced fee is believed reasonable because of the wholesale electricity use profile of distributed electrolysis plants. As in the previous case, grid electricity is evaluated at the US average fuel mix, and the average price of off-peak grid electricity is assumed to be $0.03/kW h, and the average price for intermediate and peak period grid electricity is assumed to be $0.08/kW h [38].

The comparative levelized H_2 pump prices and life cycle CO_2 findings for distributed electrolysis plants are presented in Fig. 11. The levelized H_2 pump price is 17% higher for distributed electrolysis plants using only imported pv electricity compared to centralized pv electrolysis plants with pipeline H_2 distribution. When distributed electrolysis plants increase their capacity factor by supplementing imported pv electricity with off-peak grid electricity, the levelized H_2 pump price is 15% lower than the levelized H_2 pump price for centralized pv electrolytic plants. The reduction in levelized H_2 pump price accruing from the addition of off-peak grid electricity is a function of two factors—the low cost of off-peak electricity and an increase in electrolyser operating capacity factor.

While the use of low-cost off-peak grid electricity decreases the H_2 production costs, CO_2 emissions are increased by a factor of six compared to the sole use of pv electricity. The impact of using grid electricity to supplement pv electricity on vehicle CO_2 emission is presented in Fig. 12. It should be noted that the CO_2 emissions for the distributed pv electrolysis plant model are basically identical to these findings. With the use of off-peak grid electricity, the life cycle CO_2 tailpipe emissions of H_2 vehicle are 28% lower than the tailpipe CO_2 emissions of conventional gasoline powered ICE vehicles. At higher portions of grid electricity use assuming an average US fuel mix by distributed electrolysis plants, the fuel cycle CO_2 emissions of H_2 vehicles are greater than those of conventional gasoline powered ICE vehicles.

On a final note, the effects of scale economies on levelized H_2 production cost by centralized pv electrolysis plants and distributed electrolysis plants are estimated with capital cost projections for 2007, 2010, and 2020, which are presented in Table 5. The 2007 model based is based on current price estimates for components of multi-MW pv and electrolysis plants. The 2010 model assumes a 33% reduction in pv module costs, a 10% reduction in pv power plant components, and a 10% reduction in electrolyser plant component prices, and the projections are based on a modest growth rate in component volumes above present levels. The 2020 model assumes an across the board 33% reduction in pv and electrolyser plant component prices accruing from a realization of optimized manufacturing scale for all pv and electrolyser components. The realization of optimized component manufacturing

[12] The transmission electricity losses are speculative because transmission electricity losses are contingent on a variety of factors, the most important being line voltage and transformer points. The EIA reports 9% average transmission electricity losses for the US [39]. A study conducted by Germany's DLR suggests that the long-distance transmission of electricity at distances of 2000 km and greater over high-voltage AC power lines may result in larger electricity losses [40]. The DLR transmission and transformer electricity losses for AC transmission systems are 15%/1000 km for 380 kV transmission systems, 8%/1000 km for 750 kV transmission systems, and 0.25% for each transformer station. The DLR study recommends the development of dedicated high-voltage DC (HVDC) transmission systems for the long-distance integration of large quantities of renewable electricity supplies with transmission losses of approximately 10%.

Please cite this article as: Mason JE, Zweibel K. Baseline model of a centralized pv electrolytic hydrogen system. Int J Hydrogen Energy (2007), doi: 10.1016/j.ijhydene.2006.12.019

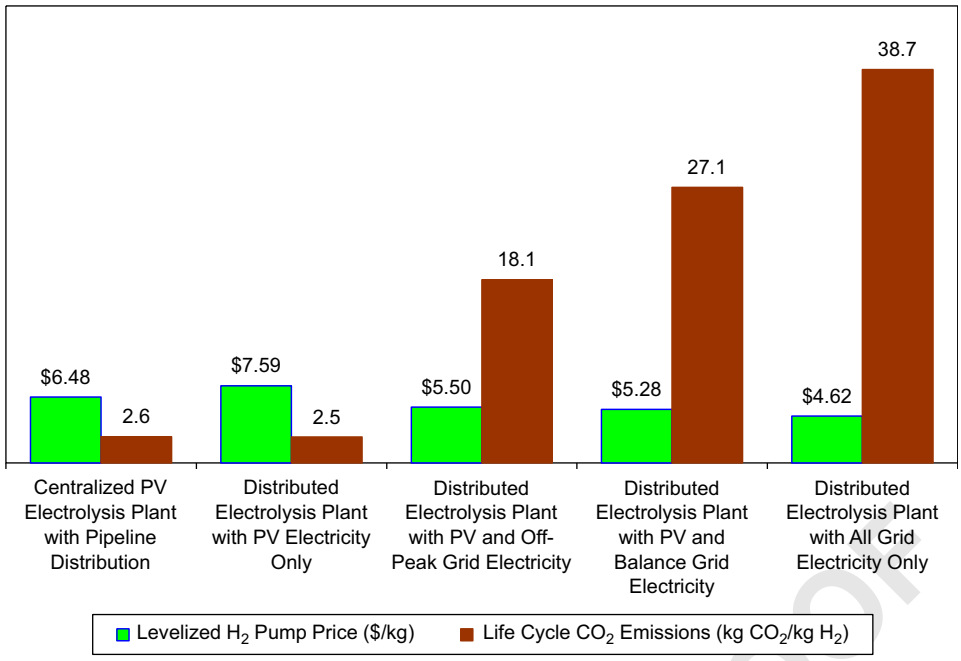

Fig. 11. Levelized H_2 prices and life cycle CO_2 emissions for distributed electrolysis plants using imported pv electricity from high insolation regions with variation in other electricity sources for the distributed electrolysis plant.

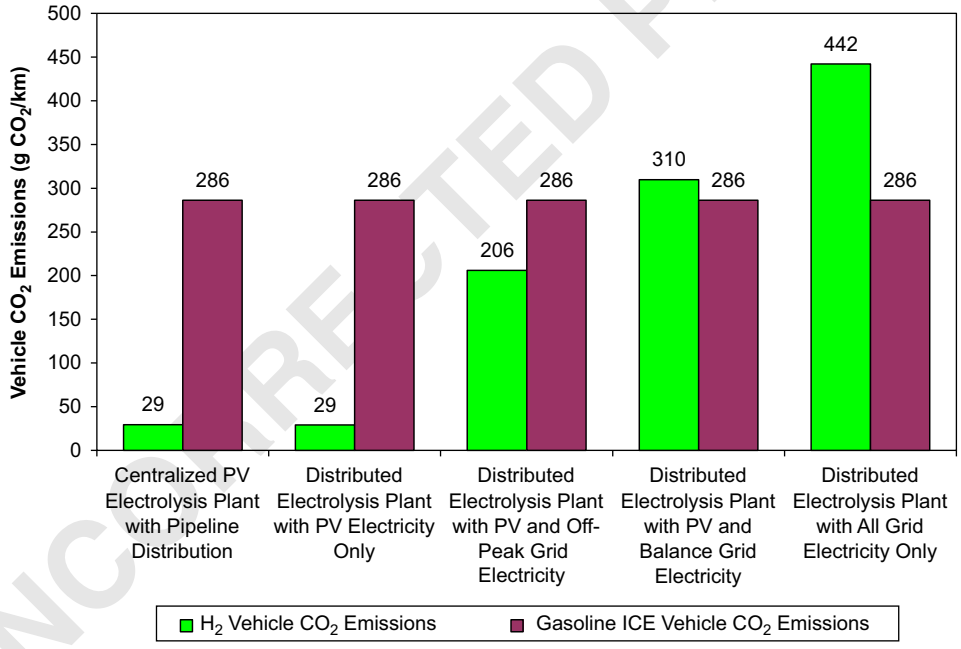

Fig. 12. Comparison of H_2 vehicle CO_2 emissions to gasoline ICE vehicle CO_2 emissions by type of electricity mix for distributed electrolysis plants.

will require a sustained growth in the deployment of systems components.

A 265-MW distributed electrolysis plant, using both imported pv and off-peak grid electricity, produces a quantity of H_2 sufficient to support the operation of 100,000 H_2 vehicles. The annual addition of one 265-MW distributed electrolysis plant, which is coupled with a 368-MW_p pv central power plant, from 2010 to 2015 is sufficient to realize the projected cost reductions in pv and electrolysis plant components. By 2020 the scale of pv electrolytic production needs to be increased by an annual addition of 10 pv electrolysis plants, which will support the annual addition of one-million H_2 vehicles. If H_2 vehicles are to be mass marketed to achieve competitive sticker prices with comparable models of conventional ICE vehicles, then the scale of pv electrolytic H_2 production is reasonable.

Please cite this article as: Mason JE, Zweibel K. Baseline model of a centralized pv electrolytic hydrogen system. Int J Hydrogen Energy (2007), doi: 10.1016/j.ijhydene.2006.12.019

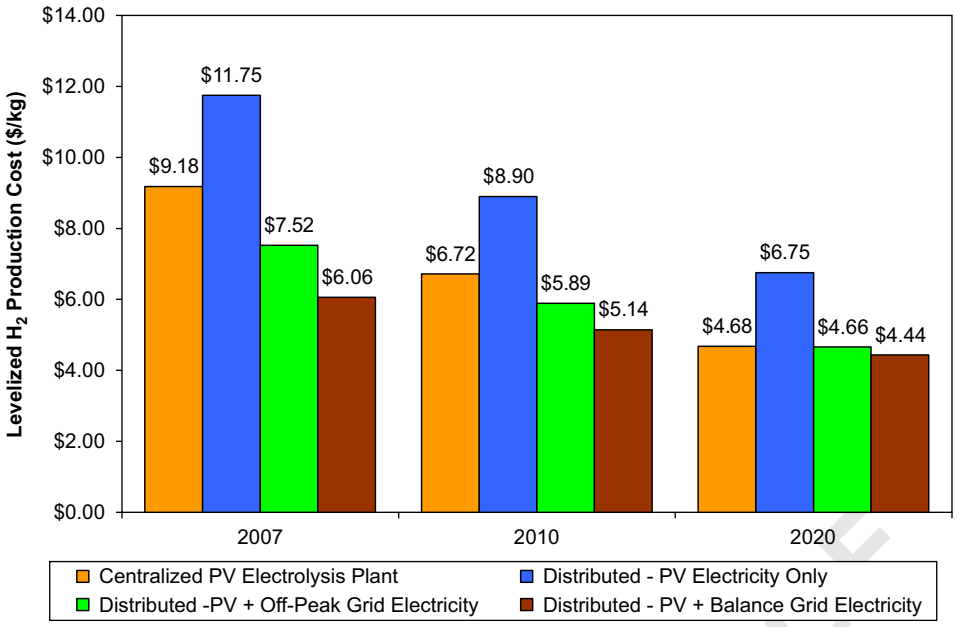

Fig. 13. Effect of scale economies on distributed electrolysis plant H_2 production cost.

The effects of increasing scale and scope economies from 2007 to 2020 on levelized H_2 pump prices are presented in Fig. 13. The levelized H_2 pump price for a one-of-a-kind pv electrolysis plant constructed at 2007 component prices is approximately 45% higher than the 2020 H_2 pump price. A significant reduction in the levelized H_2 pump price occurs with decreases in component costs from 2010 to 2020. The realization of optimized scale in the manufacture of pv components is the most important factor towards minimizing the cost of H_2 production by pv electrolysis.

In conclusion, the deployment of distributed electrolysis plants appears to be a viable option in the initial stages of H_2 production. With the development of dedicated HVDC transmission networks, the use off-peak grid electricity can be replaced with renewable electricity sources such as concentrating solar power plants and wind power plants to increase the operating capacity of distributed electrolysis plant and to reduce CO_2 emissions. The estimated 2020 levelized H_2 pump price for H_2 produced by distributed electrolysis plants using only pv, concentrating solar, and wind generated electricity is only 5–17% higher than the 2020 pump price of H_2 produced by centralized pv electrolysis plants with pipeline distribution. While distributed electrolysis plants do appear viable, it is beyond the scope of this analysis to speculate on the ultimate extent to which distributed electrolysis plants can displace pipeline H_2 distribution.

6. Conclusion

The estimated levelized H_2 pump price is $6.48/kg. Expected improvements in pv technologies will reduce the baseline H_2 pump price over time. The total capital cost of the H_2 system is $12.4 billion. While this level of capital investment is substantial, it is not without precedent. The capital investments required for a pv electrolytic H_2 production and distribution system are comparable to the capital investments to construct the cable and satellite infrastructure for the information technology industries over the past 30 years.

The total land area of the pv electrolysis plant is 260 km^2. While the land area is substantial, it is not prohibitive since pv electrolysis plants will be located in sparsely populated desert regions. Annual water consumption is 6.8-million m^3/year. This quantity of water can be supplied by on-site rain runoff collection and storage systems, imported desalinated sea water, and cogenerated desalinated water produced by CSP plants. The total life cycle energy and CO_2 emissions of delivered H_2 are 36 MJ/kg H_2 and 2.6 kg CO_2 Eq/kg H_2, respectively. The primary energy payback time is 3.1 years, and the carbon dioxide emissions payback time is 3.1 years. The replacement of gasoline powered vehicles with H_2 powered vehicles reduces both primary energy use and CO_2 emissions by 90%.

One of the most important findings is the 45–54% reduction in H_2 pump price occurring in the post-amortization, Years 31–60, H_2 production period. The Years 31–60 electrolytic H_2 production model is important, because unlike almost any other source of electricity, flat-plate, non-tracking pv has the unique attribute of very long life and very low O&M. The closest parallel is hydroelectricity, which has demonstrated the clear value of a large initial investment followed by decades of low-cost generation. The long-term reduction in H_2 price implies that pv electrolytic H_2 can be used for energy use applications other than transportation such as for centralized electricity generation and industrial applications.

Another important finding is the efficacy of deploying distributed electrolysis plants in markets distant from high insolation areas. The application of low cost, off-peak, grid electricity offsets the incremental long-distance transmission costs of pv electricity. While the use of off-peak grid electricity re-

Please cite this article as: Mason JE, Zweibel K. Baseline model of a centralized pv electrolytic hydrogen system. Int J Hydrogen Energy (2007), doi: 10.1016/j.ijhydene.2006.12.019

duces the cost of H_2 produced by distributed electrolysis plants, there is an increase in life cycle H_2 CO_2 emissions. But in terms of vehicle CO_2 emissions, the 90% reduction in vehicle CO_2 emissions contracts to a 28% reduction. The application of greater portions of grid electricity for distributed electrolysis plants result in an increase in vehicle CO_2 emissions. Post-2020 off-peak grid electricity can be replaced with electricity produced by concentrating solar power plants and wind plants. For the distributed electrolysis plant case, three issues require additional analysis—long-distance power line transmission losses, local utility fees, and extent of reduction in pipeline H_2 distribution. HVDC electricity transmission systems are being proposed for the large-scale distribution of electricity produced by renewable energy sources and may be a key component for the application of imported pv, concentrating solar power, and wind electricity for distributed electrolysis plants.

The primary challenges are the scale-up in the manufacturing capacity of pv and electrolyser components and increasing the production of tellurium and indium. The capital cost to build a multi-GW_p pv manufacturing facility is as high as $600 million [12]. The increase in tellurium and indium production will require timely investments for the addition of secondary metal production facilities, which will require coordination between pv manufacturers and metal mining and refining companies. Recycling processes for the full recovery of materials from retired pv modules need to be developed to insure the long-term supply of rare semiconductor metals. Also, further progress in the development of low-cost x-Si pv technologies is needed to insure that pv is able to realize its full potential as an energy source for global H_2 production and electricity generation.

The development of a pv electrolytic H_2 production and distribution system will provide substantial economic benefits. Growth in the pv, electrolyser, compressor and MH industries will create jobs that will be many times the number of jobs lost in the gasoline production industry. The greatest economic benefits are the mitigation of global warming impacts and the promotion of global energy sustainability.

Acknowledgement

HRI would like to thank the Solar Energy Campaign for funding to support this research.

References

[1] Yang C, Ogden J. Determining the lowest-cost hydrogen delivery mode. Int J Hydrogen Energy doi:10.1016/j.ijhydene.2006.05.009.
[2] Shi S, Hwang JY. Research frontier on new materials and concepts for hydrogen storage. Int J Hydrogen Energy doi:10.1016/j.ijhydene.2006.05.015.
[3] Jorgenson S. Taped interview. Hydrogen Forecast ⟨www.hydrogenforecast.com⟩; 2006.
[4] Harrison MR, Shires TM, Wessels JK, Cowgill RM. Methane emissions from the natural gas industry. Project summary. United States Environmental Protection Agency. Report No. 600/SR-96/080. Research Triangle Park, NC: National Risk Management Research Laboratory; 1997.
[5] Zweibel K. The terawatt challenge for thin film pv. In: Poortmans J, Archipov V, editors. Thin film solar cells: fabrication, characterization and applications. New York: Wiley; 2005.
[6] Szyszka A. Ten years of solar hydrogen demonstration project at neunburg vorm Wald, Germany. Int J Hydrogen Energy 1998;24:849–60.
[7] Cloumann A, d'Erasmo P, Nielsen M, Halvorsen BG, Stevens P. Analysis and optimisation of equipment cost to minimise operation and investment for a 300 MW electrolysis plant. Notodden, Norway and Moret sur Loing, France: Norsk Hydro Electrolysers AS and Electricité de France, Direction des Etudes et Recherches; 1994.
[8] Norsk Hydro. Personal communications with Harry Tobiassen; 2004.
[9] United States Federal Highway Administration. Highway miles traveled (Urban and Rural). Washington, DC: U.S. Department of Transportation; 2003.
[10] Marion W, Wilcox S. Solar radiation data manual for flat-plate and concentrating collectors. Manual Produced by NREL's Analytic Studies Division. Contract No. NREL/TP-463-5607, DE93018229. Golden, CO: National Renewable Energy Laboratory (NREL); April 1994.
[11] Ford Motor Company. Personal interview with Phillip Chizek, Manager, Marketing and Sales, Sustainable Mobility Technologies, Ford Motor Company; 2003.
[12] Chen Y, Wu CZ, Wang P, Cheng HM. Structure and hydrogen storage property of ball-milled $LiNH_2/MgH_2$ mixture. Int J Hydrogen Energy doi:10.1016/j.ijhydene.2005.09.001.
[13] Chao BS, Young RC, Myasnikov V, Li B, Huang B, Gingl F, et al. Recent advances in solid hydrogen storage systems. Rochester Hills, MI: Texaco Ovonic Hydrogen Systems, LLC; 2004.
[14] Keshner MS, Arya R. Study of potential cost reductions resulting from super-large-scale manufacturing of pv modules. Final Subcontract Report, NREL/SR-520-36846. Golden, CO: National Renewable Energy Laboratory; October 2004.
[15] Dietsch T. Photovoltaics of the neunburg vorm wald solar hydrogen project. Power Eng J 1996;10:17–26.
[16] Amos WA. Costs of storing and transporting hydrogen. NREL/TP-570-25106. Golden, CO: National Renewable Energy Laboratory; 1998.
[17] Copeland TE, Weston JF, Shastri K. Financial theory and corporate policy. 4th ed., Boston, MA: Addison-Wesley; 2005.
[18] Praxair. Personal communication with Joseph Schwartz; 2004.
[19] Peress J. Working with non-ideal gases: here are two proven methods for predicting gas compressibility factors. CEP Magazine 2003;March: 39–41.
[20] Mason J, Fthenakis V, Kim C, Hansen T. Life cycle energy and GHG emissions analysis of a field pv plant. Progr Photovoltaics: Res Appl 2006;14:179–90.
[21] Fthenakis V, Alsema E. Photovoltaics energy payback times, greenhouse gas emissions and external costs: 2004–early 2005. Progr Photovoltaics: Res Appl 2006;14:275–80.
[22] Weiss MA, Heywood JB, Drake EM, Schafer A, AuYeung FF. On the road in 2020: a life cycle analysis of new automobile technologies. Energy Laboratory Report # MIT EL 00-003, 2000. Cambridge, MA: Laboratory for Energy and the Environment, Massachusetts Institute of Technology; 2000.
[23] Environdec. Stockholm: Environmental Product Declarations, Swedish Environmental Management Council; 2006.
[24] Singh M. Total Energy Cycle Assessment of Electric and Conventional Vehicles: An Energy and Environmental Analysis, Volume I: Technical Report and Volume II: Appendices A-D to Technical Report. Prepared by Argonne National Laboratory National Renewable Energy Laboratory and Pacific Northwest National Laboratory. Washington, DC: U.S. Department of Energy, Office of Energy Efficiency and Renewable Energy; 1998.
[25] Wibberley L. LCA in sustainable architecture (LISA), sustainable technology, BHP Billiton technology. Melbourne: BlueScope Steel; 2002.
[26] Weiss M, Heywood JM, Schafer A, Natarajan VK. Comparative assessment of fuel cell cars. Report prepared by the Laboratory for Energy and the Environment, MIT LFEE 2003-001 RP. Cambridge, MA: Massachusetts Institute of Technology; 2003.
[27] Gaines L, Stodolsky F, Cuenca R, Eberhardt J. Life cycle analysis for heavy vehicles. In: Air and waste management association annual meeting, San Diego, CA; 1998.
[28] Wang MQ. GREET Version 1.6. Center for Transportation Research, Argonne National Laboratory. Chicago: University of Chicago; 2001.

Please cite this article as: Mason JE, Zweibel K. Baseline model of a centralized pv electrolytic hydrogen system. Int J Hydrogen Energy (2007), doi: 10.1016/j.ijhydene.2006.12.019

[29] United States Geological Survey. Annual mineral commodity summaries, U.S. Geological Survey. Washington, DC: US Department of the Interior; 2006.
[30] Sanden BA. Materials availability for thin film pv and the need for 'technodiversity.' In: EUROPV 2003, Granada, Spain; 2003.
[31] Zweibel K. The terawatt challenge for thin film pv: a work in progress, Thin film partnership, NREL. Golden, CO: National Renewable Energy Laboratory (NREL); 2006.
[32] Fthenakis VM, Fuhrmann M, Heiser J, Lanzirotti A, Fitts J, Wang W. Emissions and encapsulation of cadmium in CdTe pv modules during fires. Progr Photovoltaics: Res Appl 2005;13:1–11.
[33] Fthenakis VM. Life cycle impact analysis of cadmium in CdTe pv production. Renewable Sustainable Energy Rev 2004;8:303–34.
[34] Zweibel K. Issues in thin film pv manufacturing cost reduction. Sol Energy Mater Sol Cells 1999;59:1–18.
[35] Hein JR, Koschinsky A, Holliday AN. Global occurrence of tellurium-rich ferromanganese crusts and a model for the enrichment of tellurium. Geochim Cosmochim Acta 2003;67(6):1117–27.
[36] City of Portland. Cooling water efficiency guidebook. Bureau of Water Works. Portland, OR: City of Portland; 2005.
[37] Shinnar R, Citro F. Solar thermal energy: the forgotten energy source. Clean Fuels Institute, Department of Chemical Engineering. City College of New York; 2005.
[38] EIA. Annual Energy Outlook 2005, Market Trends—Electricity Demand and Supply, Data Table for Figure 71. Washington, DC: Energy Information Administration, U.S. Department of Energy; 2005.
[39] EIA. Annual Energy Review 2005. Washington, DC: Energy Information Administration, U.S. Department of Energy; 2005. p. 223.
[40] German Aerospace Center (DLR), Institute of Technical Thermodynamics Section Systems Analysis and Technology Assessment. Trans-Mediterranean Interconnection for Concentrating Solar Power. Bonn: Federal Ministry for the Environment, Nature Conservation and Nuclear Safety; 2006. p. 19.

Please cite this article as: Mason JE, Zweibel K. Baseline model of a centralized pv electrolytic hydrogen system. Int J Hydrogen Energy (2007), doi: 10.1016/j.ijhydene.2006.12.019